Identification of bone morphogenetic protein 7 (BMP7) as an instructive factor for human epidermal Langerhans cell differentiation

Yasmin, Nighat ; Bauer, Thomas ; Modak, Madhura ; Wagner, Karin ; Schuster, Christopher ; Köffel, Rene ; Seyerl, Maria ; Stöckl, Johannes ; Elbe-Bürger, Adelheid ; Graf, Daniel ; Strobl, Herbert

Abstract: Human Langerhans cell (LC) precursors populate the epidermis early during prenatal development and thereafter undergo massive proliferation. The prototypic antiproliferative cytokine TGF- 1 is required for LC differentiation from human CD34(+) hematopoietic progenitor cells and blood monocytes in vitro. Similarly, TGF- 1 deficiency results in LC loss in vivo. However, immunohistology studies revealed that human LC niches in early prenatal epidermis and adult basal (germinal) keratinocyte layers lack detectable TGF- 1. Here we demonstrated that these LC niches express high levels of bone morphogenetic protein 7 (BMP7) and that Bmp7-deficient mice exhibit substantially diminished LC numbers, with the remaining cells appearing less dendritic. BMP7 induces LC differentiation and proliferation by activating the BMP type-I receptor ALK3 in the absence of canonical TGF- 1-ALK5 signaling. Conversely, TGF- 1-induced in vitro LC differentiation is mediated via ALK3; however, co-induction of ALK5 diminished TGF- 1-driven LC generation. Therefore, selective ALK3 signaling by BMP7 promotes high LC yields. Within epidermis, BMP7 shows an inverse expression pattern relative to TGF- 1, the latter induced in suprabasal layers and up-regulated in outer layers. We observed that TGF- 1 inhibits microbial activation of BMP7-generated LCs. Therefore, TGF- 1 in suprabasal/outer epidermal layers might inhibit LC activation, resulting in LC network maintenance.

DOI: https://doi.org/10.1084/jem.20130275

Identification of bone morphogenetic protein (BMP) 7 as an instructive factor for human epidermal Langerhans cell differentiation

Nighat Yasmin[1,2], Thomas Bauer[1,2], Madhura Modak[1], Karin Wagner[4], Christopher Schuster[3], Rene Köffel[1,2], Maria Seyerl[1], Johannes Stöckl[1], Adelheid Elbe-Bürger[3], Daniel Graf[5] and Herbert Strobl[1,2]

[1] Institute of Immunology, Center of Pathophysiology, Infectiology and Immunology, Medical University of Vienna, Austria, [2] Institute of Pathophysiology and Immunology, Center of Molecular Medicine, Medical University Graz, Austria, [3] Department of Dermatology, Division of Immunology, Allergy and Infectious Diseases, Laboratory of Cellular and Molecular Immunobiology of the Skin, Medical University of Vienna, Austria, [4] Center for Medical Research, Medical University Graz, Austria, [5] Orofacial Development and Regeneration, Institute of Oral Biology, Center for Dental Medicine, University of Zurich, Zurich, Switzerland.

Running Title: BMP7 induces LC differentiation.

Caption: Bone morphogenetic protein (BMP) 7 promotes the differentiation of Langerhans cells in the epidermis during prenatal development.

Corresponding author: Herbert Strobl, MD, Institute of Immunology, Center of Pathophysiology, Infectiology and Immunology, Medical University of Vienna, Vienna Competence Center, 1090, Vienna, Austria. Phone number: +43-6767576195, Fax number: +43-1-40160-933201 Email: herbert.strobl@meduniwien.ac.at

Abstract word count: 191

Text character count (no spaces): 34211

Figure count: 8

Supplementary Table count: 2

Reference count: 59

Non Standard Abbreviations:

EGA	Estimated gestational Age
IRES	Internal Ribosome Entry Site
ALK	Activin Like Kinase
BMP	Bone Morphogenetic Protein
wk	Week
TARC	Thymus and activation regulated chemokine

ABSTRACT

Human Langerhans cell (LC) precursors populate the epidermis early during prenatal development and thereafter undergo massive proliferation. The prototypic anti-proliferative cytokine TGF-β1 is required for LC differentiation from human $CD34^+$ hematopoietic progenitor cells and blood monocytes *in vitro*. Similarly, TGF-β1 deficiency results in LC loss *in vivo*. However, immunohistology studies revealed that human LC niches in early prenatal epidermis and adult basal (germinal) keratinocyte layers lack detectable TGF-β1. Here we demonstrated that these LC niches express high levels of BMP7 and that Bmp7-deficient mice exhibit substantially diminished LC numbers, with the remaining cells appearing less dendritic. BMP7 induces LC differentiation and proliferation by activating the BMP type-I receptor ALK3 in the absence of canonical TGF-β1-ALK5 signaling. Conversely, TGF-β1-induced *in vitro* LC differentiation is mediated via ALK3; however, co-induction of ALK5 diminished TGF-β1-driven LC generation. Therefore, selective ALK3 signaling by BMP7 promotes high LC yields. Within epidermis, BMP7 shows an inverse expression pattern relative to TGF-β1, the latter induced in suprabasal layers and upregulated in outer layers. We observed that TGF-β1 inhibits microbial activation of BMP7-generated LCs. Therefore, TGF-β1 in suprabasal/outer epidermal layers might inhibit LC activation resulting in LC network maintenance.

INTRODUCTION

LCs form dense cellular networks in basal/suprabasal layers of stratified epidermal and mucosal tissues. LCs are considered as the environmentally exposed outposts of the immune system. They are capable of recognizing microbes and environmental substances and provide first line innate anti-viral immune defense. Moreover, they are capable of migrating to skin-draining lymph nodes, and of inducing T cell-mediated adaptive immune responses to antigens encountered in the epidermis. This unique epidermal dendritic cell (DC) subset is developmentally dependent on the cytokine TGF-β1 as evidenced from *in vitro* and *in vivo* data (Igyarto and Kaplan, 2012; Romani et al., 2012).

TGF-β1 was identified as a factor inducing LC differentiation from human monocytopoietic cells *in vitro* (Strobl et al., 1996). While in the absence of TGF-β1, cytokine stimulated $CD34^+$ hematopoietic progenitor cells (HPCs) developed into monocyte/macrophages, supplementation of these cultures with TGF-β1 directed progenitor cell differentiation towards LCs (Strobl et al., 1997; Strobl et al., 1996). In line with this, neutralizing anti-TGF-β1 antibody abrogated LC differentiation (Caux et al., 1999) demonstrating that endogenous TGF-β1 in these cultures (Caux et al., 1992) is required for the induction of LC differentiation. Congruent with these observations, blood monocytes acquire LC characteristics in response to TGF-β1 stimulation (Geissmann et al., 1998; Hoshino et al., 2005). Murine *in vivo* data similarly demonstrated that LC differentiation depends on TGF-β1. LC networks are absent from TGF-$\beta1^{-/-}$ mice (Borkowski et al., 1996) and the specific deletion of TGF-β1 and TGF-βRII in LCs resulted in reduced numbers of epidermal LCs, indicating that TGF-β1 acts directly on LC differentiation (Kaplan et al., 2007). Congruent with these observations, LC networks were impaired in mice deficient for TGF-β1 downstream signaling molecules Id2 (Hacker et al., 2003) and Runx3 (Fainaru et al., 2004). Together, these observations firmly established a key role of TGF-β1 during LC differentiation.

Recent data however challenged the view that TGF-β1 is required for LC differentiation. First, LCs possess substantial proliferative capacity in the steady state (Merad et al., 2002) as well as during prenatal life or during inflammation (Chang-Rodriguez et al., 2005; Chorro et al., 2009; Schuster et al., 2009). These findings seem to be incompatible with the well-defined anti-proliferative function of TGF-β1 (Dennler et al., 2002). Second, basal keratinocyte layers are devoid of TGF-β1 expression, which has been considered critical for keratinocyte stem cell proliferation (Li et al., 2006). Some LCs reside in basal keratinocyte layers and Ki67 staining

revealed that a fraction of these cells undergo proliferation in the steady-state adult skin (Schuster et al., 2009). Third, LC precursor seeding of the prenatal epidermis precedes TGF-β1 expression induction in the epidermis. (Schuster et al., 2009). Fourth, the deletion of components of the canonical TGF-β1 signaling cascade still allowed normal LC differentiation *in vivo*. Canonical TGF-β1 signaling is transmitted via the type-I receptor ALK5 and also depends on type-II receptors, leading to the downstream activation of transcription factors Smad2/3 (Massague, 1998). Deficiency of Smad3 failed to impair LC networks (Ying-Ping Xu, 2012). Similarly, the deletion of ALK5 from $CD11c^+$ or $CD207^+$ cells allowed LC differentiation as revealed from the presence of LC networks at birth; only postnatally LC numbers rapidly dropped due to the emigration of LCs from the epidermis to lymph nodes shortly after birth (Kel et al., 2010; Zahner et al., 2011). Consistently, the conditional deletion of TGF-β1 and TGF-βRII in LCs resulted in their migration to the lymph nodes likely due to enhanced pro-inflammatory cytokine production and LC activation (Bobr et al., 2012). TGF-β1 also interferes with the maturation and pro-inflammatory cytokine production by monocyte-derived DCs (Geissmann et al., 1999). Taken together, canonical TGF-β1-ALK5-Smad3 signaling seems to be critical for postnatal LC network maintenance but does not seem to be required for LC differentiation.

While ALK5 is regarded as the classical TGF-β1 receptor, TGF-β1 can also activate other type-I receptors such as ALK1 (Goumans et al., 2002; Oh et al., 2000), ALK2 and ALK3 (Daly et al., 2008; Ebner et al., 1993). ALK receptors form hetero- and homo-oligomers that are differentially activated by members of the TGF-β/BMP superfamily (Miyazono et al., 2010). Considering the above mentioned recent observations that TGF-β1 might not be critical for LC differentiation, we considered deciphering the mechanism underlying LC differentiation to be of major importance. We here identified BMP7 as a key factor inducing LC differentiation.

RESULTS

TGF-β1 promotes LC differentiation through the type-I receptor ALK3.

TGF-β1 is the classical ligand for ALK5 while ALK2 and ALK3 receptors are activated by both TGF-β1 (Daly et al., 2008) and bone morphogenetic proteins (BMPs) (Miyazono et al., 2010). We aimed to explore the downstream signaling mechanism governing TGF-β1-dependent LC differentiation. Hence, we added or not inhibitors of ALK4/5/7 (SB421543) or ALK2/3/6 (dorsomorphin) to LC generation cultures. $CD34^+$ cells were pretreated for 1 hour with either compound and were subsequently induced to differentiate into LCs in the presence of GM-CSF, SCF, TNF, FLT3L and TGF-β1. Without inhibitors, a fraction of day 3 generated cells readily exhibited LC phenotypic characteristics ($CD1a^+CD207^+$). Unexpectedly, ALK5 inhibition led to the generation of increased percentages of LCs, indicating that the canonical TGF-β1/ALK5 downstream signaling is not only dispensable for LC generation but even negatively affects it (Figure 1A, left panel). In sharp contrast, interference with ALK2/3/6 receptor signaling strongly impaired LC generation, as evidenced by a substantial drop in percentages of LCs (Figure 1A, right panel). Consistently, the total numbers of day 7-generated LCs were higher in the presence of the ALK5 inhibitor in all three experiments analyzed (Figure 1B). In comparison, day 7 cultures in the presence of ALK2/3 inhibitor did not contain any viable cells (data not shown), indicating that ALK2/3 signaling rather than ALK5 is critical for TGF-β1-dependent LC differentiation from progenitor cells.

To confirm these data, we transduced $CD34^+$ cells with retroviral vectors encoding ALK2-, ALK3-, ALK5-IRES-GFP or empty control vector. Subsequently, we generated LCs from $CD34^+$ cells as previously reported (Strobl et al., 1997). GFP^+ gated cells were analyzed for LC characteristics. ALK3-transduced cells contained significantly higher percentages of $CD207^+CD1a^+$ cells as compared with empty control vector transduced cells. Moreover, neither ectopic ALK2 nor ALK5 resulted in altered percentages of LCs (Figure 1C). Together with the observation that ALK3 is expressed in the epidermis (Botchkarev et al., 1999; Hwang et al., 2001), our loss and gain of function experiments indicate that TGF-β1 utilizes ALK3 signaling for promoting LC differentiation.

LC generation cultures contained only very low percentages of cells expressing CD11b and/or CD14, that did not change significantly in response to addition of ALK inhibitors (Figure 1A). Moreover, ectopic ALK3 expression failed to promote the generation of cells expressing CD14, CD11b or the early myeloid marker myeloperoxidase (MPO) in LC generation cultures (Figure 1D). Similarly, ectopic ALK3 neither modulated percentages of cells exhibiting a $CD11b^+CD1a^+CD207^-$ monocyte-derived DC (moDC) phenotype nor a $CD14^+CD11b^+$

monocyte/macrophage phenotype generated in specific cytokine combinations (Figure 1D). Therefore, ALK3 specifically promoted the generation of $CD1a^{+}CD207^{+}$ LCs among the various cell subsets analyzed.

BMP7 is detectable in the basal epidermal layer during human prenatal development.

Among various ALK3 ligands, only BMP7 has a predominant expression pattern in basal keratinocyte layers (Takahashi and Ikeda, 1996). Moreover, only BMP7 is strongly expressed in fetal epidermis at day 17.5 p.c. (Helder et al., 1995), a time window when LC precursors first appear in the fetal murine epidermis (Chang-Rodriguez et al., 2005; Chorro et al., 2009; Elbe et al., 1989; Romani et al., 1986). However, human data on the distribution of BMP7 among keratinocyte layers during prenatal development were lacking. We previously identified proliferating LCs in basal layers of human epidermis (Schuster et al., 2009) and demonstrate here that BMP7 is detectable in the epidermis from the earliest time point analyzed (8-10 weeks EGA, Figure 2A). Stratified epidermis at subsequent time points (11-14 weeks EGA, adult) contains BMP7 exclusively in basal/suprabasal layers (Figure 2A). In comparison, TGF-β1 cannot be detected in the epidermis at 8 wk EGA (Figure 2B) (Schuster et al., 2009). Moreover TGF-β1 is undetectable in the basal epidermal layer and is only found suprabasally (Figure 2B) (Kane et al., 1990; Schuster et al., 2009). Therefore, we conclude that BMP7 expression precedes TGF-β1 expression during embryonic epidermal development and both molecules show an inverse expression pattern in the stratified epidermis: TGF-β1 exclusively suprabasally and BMP7 in the basal/germinative layer (Figure 2B). Given that epidermal LC precursors can be detected at 8-11 weeks EGA (Schuster et al., 2009) and reside in basal/suprabasal keratinocyte layers, these cells are primarily exposed to a $BMP7^{+}TGF\text{-}\beta1^{-}$ microenvironment. Only LCs in suprabasal epidermal layers are also exposed to TGF-β1.

Numeric and morphologic LC impairment in Bmp7 deficient mice.

To study the potential role of BMP7 during LC differentiation *in vivo*, we analyzed Bmp7 deficient mice (Zouvelou et al., 2009). These mice die shortly after birth limiting the analysis of the LC differentiation process. However, IA/ IE positive LCs can be already detected right after birth (P0) (Chorro et al., 2009). To assess the expression pattern of BMP7, epidermal sheets from Bmp7-LacZ mice were stained with X-gal. Widespread expression of BMP7 in murine keratinocytes was detected (Figure 3A) similar to human epidermal sections as shown in Figure 2. Epidermal LC precursor cells acquire MHCII around birth (P0) with detectable langerin/CD207 expression appearing at P2 (Chorro et al., 2009). We therefore analyzed mice at P0 using antibodies against IA/IE (MHCII). Bmp7-deficient mice (P0) showed substantial

reductions in epidermal MHCII$^+$ cell frequencies (Figure 3B). Interestingly, the MHCII$^+$ cells in these mice exhibited lower numbers of dendritic processes compared to cells from wild type littermate controls (Figure 3C).

BMP7-dependent activation of ALK3-Smad1/5/8 promotes LC differentiation.

Considering the above described *in vitro* and *in vivo* observations, we hypothesized that BMP7 might act as TGF-β1-independent positive regulator of LC differentiation and that the selective triggering of ALK3 by BMP7 might enable amplified LC generation. Hence we added BMP7 instead of TGF-β1 to LC generation cultures and monitored percentages and total numbers of LCs. A hallmark characteristic of TGF-β1-induced *in vitro* generated LCs is the formation of huge macroscopically visible homotypic E-cadherin-mediated LC clusters (Figure 4A). Strikingly, BMP7 alone induces higher frequencies of LC clusters as well as on average higher percentages of E-cad$^+$CD1a$^+$CD207$^+$ cells than TGF-β1 when added to these cultures (Figure 4A). Accordingly, total numbers of CD1a$^+$E-cad$^+$CD207$^+$ cells were significantly higher in BMP7 than in TGF-β1-supplemented cultures (Figure 4A). Therefore, BMP7 by far exceeds TGF-β1 in promoting LC generation. These observations are congruent with the above-described positive role of ALK3 in LC differentiation and with the observations that ALK5 (induced by TGF-β1 but not BMP7) inhibits LC generation. CFSE-labeling experiments confirmed superior proliferation of cells from BMP7-supplemented cultures relative to TGF-β1-treated cells (Figure 4B-C).

In subsequent experiments we performed a side-by-side comparison of BMP7 with other BMPs known to be expressed in the adult epidermis (i.e. BMP2, BMP4 and BMP6 (Botchkarev, 2003). Dose response experiments revealed that only BMP4 replaced BMP7 in inducing LC differentiation. Conversely, neither BMP2 nor BMP6 induced LC generation (data not shown). Immunohistology revealed that BMP4 is not detectable in human prenatal epidermis (data not shown) consistent with the fact that BMP4 expression can not be detected in interfollicular epidermis (Bitgood and McMahon, 1995; Lyons et al., 1989).

In subsequent experiments, we treated LC precursors with either TGF-β1 or BMP7 and analyzed the phosphorylation of Smad proteins. TGF-β1 induces phosphorylation of Smad2/3 (a signature of TGF-β signaling via ALK5) and Smad1/5/8 (a signature of canonical BMP signaling via ALK2/3) (Feng and Derynck, 2005; Schmierer and Hill, 2007). Conversely, BMP7 resulted in Smad1/5/8 phosphorylation only (Izumi et al., 2006) (Figure 5A). We next determined the expression levels of ALK 2, 3 and 5 receptors in TGF-β1-LCs or BMP7-LCs by qRT-PCR analysis during LC differentiation. TGF-β1-generated LCs exhibit higher expression levels of ALK5 than ALK3. Conversely, an inverse expression pattern was observed for BMP7-generated

LCs (ALK3>ALK5) (Figure 5B). TGF-β1 is known to be auto-induced by canonical TGF-β1-ALK5 signaling. Accordingly, TGF-β1 mRNA was induced in TGF-β1-supplemented LC generation cultures. Conversely, BMP7-supplemented LC generation cultures did not exhibit induction of TGF-β1 mRNA (Figure 5C). These observations are consistent with our finding that LC differentiation occurs independently of ALK5/Smad2/3 signaling.

BMP7-generated LCs produce higher amounts of pro-inflammatory cytokines in response to microbial signals than TGF-β1-generated LCs.

TGF-β1 inhibits pro-inflammatory cytokine production and DC maturation (Geissmann et al., 1999). Accordingly, ALK5 deficiency in LCs resulted in their spontaneous egress from the postnatal epidermis and this effect was accompanied by LC activation/maturation (Kel et al., 2010). We analyzed whether BMP7-ALK3-dependent LCs show enhanced cytokine production relative to TGF-β1-induced LCs. LCs generated in the presence of BMP7 or TGF-β1 form large clusters allowing enrichment of E-cad^{+}CD1a^{+}CD207^{+} LCs using 1g-sedimentation (Figure 6A) (Gatti et al., 2000). LCs generated under both conditions, showed similar upregulation of T cell co-stimulatory molecules CD86 and CD83 in response to TLR ligands peptidoglycan (PGN) and Pam3CSK4 (Figure 6B). However, PGN-treated BMP7 LCs produced substantially higher amounts of proinflammatory cytokines (TNF, IL-1β, IL-6, IL-12p40 and IL-12p70) along with higher levels of immunosuppressive cytokine IL-10 compared with TGF-β1 LCs (Figure 6C). In the absence of TLR ligand, BMP7- or TGF-β1-generated LCs exhibited similar low expression levels of pro-inflammatory cytokines (Figure 6C).

Moreover, TLR-stimulated BMP7-generated LCs possessed higher allogeneic T cell immunostimulatory capacity than TGF-β1-generated LCs in 12 out of 14 independent experiments (Figure 6D). Additionally, these two LC populations differed in the induction of T helper (Th) responses from adult allogeneic T cells. Specifically, TGF-β1-LCs expressed high levels of the Th2-type chemokine thymus and activation-regulated chemokine (TARC)/CCL17 than BMP7-LCs. Consistently, TGF-β1-LCs induced T cells producing higher amounts of IL-13 and IL-5 (affiliated with Th2 responses); vice versa BMP7 LCs induced higher amounts of IFNγ (affiliated with Th1 responses) (Figure 6E and F). Lower cytokine production from cord blood T cells as compared to adult peripheral blood T cells (Figure 6F) is in line with previous observations (Gupta et al., 2005).

Genome wide analysis shows similar gene expression by TGF-β1-LCs and BMP7-LCs.

To rule out that the above-described differences in cytokine production and T cell stimulation of TGF-β1-LCs versus BMP7-LCs are due to differences in cell lineage identity, we performed

genome-wide cDNA microarray analyses of flow sorted $CD1a^+CD207^+$ cells. Both populations clustered together in terms of gene expression pattern observed in three independent experiments (Figure 7, donors A, B, C). Moreover, comparison with recently deposited data sets (Hutter et al., 2012; Lundberg et al., 2013) revealed a closer resemblance to *ex vivo* isolated human LCs (Hutter et al., 2012) than to $CD34^+$ cell-derived LCs described in a recent study (Lundberg et al., 2013). This latter study used a different cytokine combination to generate LCs (i.e. IL-4 instead of FLT3L) potentially explaining the observed differences. For example, it was previously reported that IL-4 antagonizes the induction of certain TGF-β1-induced LC marker characteristics when added to cultures of $CD34^+$ progenitor cells containing GM-CSF and TNF (Caux et al., 1999).

Late addition of TGF-β1 to BMP7 supplemented cultures enhances percentages of $CD207^+CD1a^+$ LCs.

Whereas percentages of $CD207^+CD1a^+$ cells generated in the presence of TGF-β1 or BMP7 were equivalent, total cellularity was much higher in BMP7- than in TGF-β1-supplemented cultures (Figure 4A). We observed that BMP7-supplemented cultures contain markedly higher percentages of $CD1a^+E\text{-}cad^+$ cells that lacked CD207 (Figure 4A). Large percentages of these cells positively correlated with larger LC cluster numbers present in these cultures indicating that these cells may represent immediate precursors of LCs still capable of proliferation. Thus, we hypothesized that TGF-β1 might inhibit cell cycle progression, in turn allowing terminal LC differentiation, similarly as previously observed for erythropoiesis (Krystal et al., 1994). Hence, we analyzed whether $CD1a^+E\text{-}cad^+CD207^-$ cells from BMP7 LC generated cultures can be induced to differentiate into $CD1a^+E\text{-}cad^+CD207^+$ cells by the late addition of TGF-β1. Adding TGF-β1 to BMP7 LC generation cultures at day 5 indeed resulted in higher percentages of $CD1a^+E\text{-}cad^+CD207^+$ cells within 48 h and this effect was accompanied by diminished percentages of $CD1a^+E\text{-}cad^+CD207^-$ cells. Using this two-step culture system (BMP7, 5 days, followed by TGF-β1 for 48 h), very high numbers of $CD1a^+E\text{-}cad^+CD207^+$ LCs were generated (Figure 8A). The first culture phase (BMP7-supplemented; no TGF-β1) can be prolonged from 5 to 7 days (data not shown). Conversely, when TGF-β1 was added at day 0 to BMP7-supplemented cultures, similar cellularity and percentages of LCs were observed as for TGF-β1 alone (data not shown). Therefore, TGF-β1 effects dominate over BMP7 effects on cell proliferation in LC generation cultures.

BMP7 strongly promotes LC generation in serum-free medium devoid of TNFα and SCF.

Given the strong effect of BMP7 on LC generation, we asked in subsequent experiments whether BMP7 signaling might allow elimination of other cytokine stimuli present in this culture model. Therefore, the above-mentioned two-step protocol was used for cytokine omission experiments. Specifically, we analyzed consequences of omission of individual or combinations of cytokines from the first culture phase. The omission of FLT3L led to substantially decreased percentages and numbers of LCs. Conversely, omission of both TNF and SCF - two factors that were previously shown to be critical for LC generation (Caux et al., 1992; Young et al., 1995) - did not affect LC generation (Figure 8B). Therefore, a cytokine combination containing BMP7, GM-CSF and FLT3L, followed by TGF-β1 for the final 48 h efficiently induces the generation of $CD207^{+}CD1a^{+}$ LCs from progenitor cells. In conclusion, the addition of BMP7 allows the elimination of two critical cytokines from previously optimized LC generation protocols.

TGF-β1 inhibits pro-inflammatory cytokine production by BMP7-generated LCs.

While TGF-β1 generated LCs produce much lower levels of pro-inflammatory cytokines than BMP7 generated LCs in response to microbial stimuli (Figure 6C), LCs generated by using the sequential protocol (6 days BMP7, followed by 48 h TGF-β1) equaled LCs from TGF-β1 supplemented LC generation cultures (Figure 8C). Therefore, TGF-β1 strongly impairs pro-inflammatory cytokine production from BMP7-generated LCs.

DISCUSSION

LCs reside within basal and suprabasal epidermal layers in adult human skin. During prenatal development, already the single layered epidermis is populated by LC precursors and undergoes considerable proliferation to allow a tight LC network formation before birth. Also in adult epidermal basal layers, a small portion of LCs proliferates as evidenced by the expression of Ki67 (Schuster et al., 2009). We here showed that LCs entering the epidermis are initially exposed to a BMP-7^{hi} environment. BMP7 is strongly expressed in embryonic epidermis at 8 weeks EGA, a time point when LC precursors are first detectable in human embryonic skin. In stratified epidermis in fetal and adult skin, BMP7 expression is restricted to basal and suprabasal keratinocyte layers, but is lost in outer epidermal layers. Inversely, TGF-β1 is induced in suprabasal layers only and is upregulated in outer epidermal layers (Kane et al., 1990; Schuster et al., 2009). Therefore, TGF-β1 shows a reciprocal distribution versus BMP7 in the epidermis. Consistently, BMP7 expression (EGA week 8) precedes TGF-β1 induction (EGA week 11, restricted to outer keratinocyte layers) during fetal epidermal development.

We further demonstrated that BMP7 induces LC differentiation accompanied by massive cell proliferation *in vitro*. Conversely, TGF-β1 inhibited LC activation and proliferation dominantly when added to BMP7-dependent LC generation cultures. BMP7 activates ALK3 (canonical BMP signaling) in the absence of ALK5 (canonical TGF-β1 signaling). On the contrary, TGF-β1 activates both cascades. We showed by gain and loss of function studies that ALK3 signaling promotes LC differentiation. Together, here presented data indicate that LC differentiation and proliferation is induced by BMP7-ALK3 in the absence of canonical TGF-β1-ALK5 signaling. Instead, canonical TGF-β1-ALK5 signaling has an important role for the maintenance of LC networks after birth (Kel et al., 2010). We showed that the addition of TGF-β1 to BMP7-generated LCs inhibits TLR-mediated LC activation. Since the epidermis is populated with commensal bacteria immediately after birth, TGF-β1 in suprabasal/outer epidermal layers might inhibit LC activation, which in turn may secure LC network maintenance.

TGF-β1 inhibits LC activation at least in part by inducing negative signaling proteins such as Axl (Bauer et al., 2012) which contribute to low pro-inflammatory cytokine production in LCs. In support for this model, *in vitro* BMP7 generated LCs lacked Axl (T. Bauer, unpublished observations). Moreover, basal keratinocyte layers and LCs located in basal layers lacked Axl, thus demonstrating that Axl possesses a similar epidermal expression distribution as observed for TGF-β1 (Bauer et al., 2012). Consistently, a portion of *ex vivo* isolated LCs lacked

Axl (Bauer et al., 2012). The finding that only a portion of murine LCs show activation of Smad2/3 proteins (Bobr et al., 2012) is in line with the here proposed model that TGF-β1 is constitutively active only in a subset of LCs.

Four members of the BMP family can be detected in the epidermis (BMP2, BMP4, BMP6, BMP7) (Botchkarev, 2003). Among them, only BMP7 is expressed at high levels in basal keratinocyte layers. Moreover we demonstrated here that BMP7 is strongly expressed in single-layered fetal epidermis at 8 weeks EGA, a time point when LC precursors are first detectable in the epidermis. Our study is to our knowledge the first to show that BMP7 expression is detectable in basal/suprabasal epidermal layers during human prenatal development. In comparison, BMP6 is absent or only very weakly expressed in basal keratinocyte layers and its expression correlates positively with increased keratinocyte differentiation (Lyons et al., 1989), similarly as shown for TGF-β1 (Bascom et al., 1989; Keski-Oja and Koli, 1992). It was previously noted that BMP7 and BMP6 exhibit opposite expression distribution among murine epidermal keratinocyte layers (Lyons et al., 1989; Takahashi and Ikeda, 1996). The other BMPs i.e. BMP2 and BMP4 are predominantly expressed in the hair follicle epithelium and mesenchyme, but not or only weakly in interfollicular epidermis (Bitgood and McMahon, 1995; Lyons et al., 1989).

Bmp7 KO mice exhibited substantially reduced numbers of LCs with the remaining LCs being morphologically less “dendritic” as compared to LCs from wild type littermates. Therefore we here described non-redundant positive effects of BMP7 on LC differentiation *in vivo*. Our data however do not rule out that other BMPs/type-1 receptor agonists may exert (partial) redundancy with BMP7 in promoting LC differentiation. The observations that epidermal transgenic expression of the BMP/activin inhibitor follistatin reduces LC numbers (Stoitzner et al., 2005) are consistent with a major role of the BMP-ALK3-Smad1/5/8 pathway in LC differentiation *in vivo*.

Our mechanistic insights into LC differentiation allowed us to design a greatly improved protocol for LC generation from $CD34^+$ hematopoietic progenitor cells in serum-free medium. Side-by-side analysis revealed that BMP7-supplemented cultures by far exceed TGF-β1-supplemented cultures in terms of absolute numbers of generated LCs as revealed from LC cluster formation and immuno-phenotypic analyses. Therefore BMP7 signaling is sufficient to induce LCs. Additionally, BMP7 allowed to eliminate two other cytokines (i.e. SCF and TNF) from optimized LC generation cultures. Thus, a combination of only three cytokines, i.e. GM-CSF, FLT3L and BMP7 with the late addition of TGF-β1 for 48 h was found optimal for generating high yields of LCs. We showed that TGF-β1 induces LC generation via ALK3. However, the co-activation of ALK5 led to a reduction of LC generation. As a net effect, this led

to only limited amounts of LC generation in previously optimized TGF-β1-dependent differentiation cultures of $CD34^+$ cells. A key finding of our study was that the replacement of TGF-β1 by BMP7 allows circumventing ALK5-mediated proliferation inhibition observed by TGF-β1. Consequently, BMP7 allows the generation of high numbers of LCs. Nevertheless, the late addition of TGF-β1 for the final 48 h was beneficial since it led to elevated percentages of generated LCs, potentially due to a negative effect of TGF-β1 on cell proliferation. Additionally, late TGF-β1 led to inhibition of TLR-mediated pro-inflammatory cytokine production by LCs. On the other hand, BMP7-generated LCs not exposed to TGF-β1 were highly potent inducers of T cell proliferation. This differential requirement might reflect in vivo niches and could help to explain differential T cell responses depending on the site of LC activation. In support of this concept, BMP7-LCs and TGF-β1-LCs differed in provoking Th1 versus Th2 responses *in vitro*. Moreover, this newly developed BMP7-dependent LC generation procedure with or without late TGF-β1 might be of interest for inducing strong anti-viral/anti-tumor T cell responses.

In conclusion, we here provide a mechanistic model for LC differentiation that utilizes two different family members of the TGF-β/BMP superfamily: BMP7 induces LC differentiation and proliferation whereas TGF-β1 secures low levels of cytokine production by differentiated LCs, a potential prerequisite for postnatal LC network maintenance and function.

MATERIALS AND METHODS

Isolation of cells.

Cord blood samples were collected during healthy full-term deliveries. Approval was obtained from the Medical University of Vienna institutional review board for these studies. Informed consent was provided in accordance with the Declaration of Helsinki. $CD34^+$ cells were isolated as previously described (Taschner et al., 2007).

Cytokines and Reagents.

Human stem-cell factor (SCF), thrombopoietin (TPO), tumor necrosis factor alpha (TNF), granulocyte-macrophage colony-stimulating factor (GM-CSF), fms-related tyrosine kinase 3 ligand (FLT3L, interleukin-4 (IL-4), interleukin-6 (IL-6) and bone morphogenetic proteins (BMP4 and BMP6) were purchased from PeproTech (London, United Kingdom); transforming growth factor beta 1 (TGF-β1) was purchased from R&D Systems (Wiesbaden, Germany). BMP7 and BMP2 were purchased from ImmunoTools (Friesoythe, Germany). ALK4/5/7 inhibitor (SB431542) and ALK2/3/6 inhibitor (dorsomorphin dihydrochloride) were purchased from, Tocris biosciences (Bristol, UK).

In vitro culture of $CD34^+$ cord blood hematopoietic stem cells.

$CD34^+$ cells were cultured for 2-3 days under progenitor expansion conditions (FLT3L, SCF and TPO, each at 50 ng/ml) in serum-free medium (X-VIVO 15 medium, Bio Whittaker, Walkersville, MD) before subculturing with lineage specific cytokines. LC cultures were described before (Strobl et al., 1997). In brief, pre-expanded $CD34^+$ cells (2 - 4×10^4/ml per well) were cultured in 24-well tissue culture plates in serum-free CellGro DC medium (CellGenix) supplemented with GM-CSF (100 ng/ml), SCF (20 ng/ml), FLT3L (50 ng/ml), TNF (2.5 ng/ml), and TGF-β1 (0.5 ng/ml) for 7 days. Cultures were supplemented with 2.5 mM GlutaMax (Gibco/Invitrogen) and 125 U/ml each penicillin/streptomycin. LC clusters were purified as previously described (Gatti et al., 2000). For moDC generation, pre-expanded $CD34^+$ cells (2 - 4×10^4/ml per well) were first cultured in 24-well plate in CellGro DC medium (CellGenix) supplemented with 10% FCS in the presence of GM-CSF (100 ng/ml), SCF (20 ng/ml), FLT3L (50 ng/ml) and TNF (2.5 ng/ml) for 4 days, followed by GM-CSF (100 ng/ml) and IL-4 (25 ng/ml) for 3 days in RPMI+10% FCS medium (Jurkin et al., 2010). For monocyte/macrophage (Mϕ) generation, pre-expanded $CD34^+$ cells (2 - 4×10^4/ml per well) were cultured in 24-well plate in the presence of M-CSF (100 ng/ml), IL-6 (20 ng/ml), FLT3L (50 ng/ml) and SCF (100 ng/ml) in RPMI+10% FCS medium (Heinz et al., 2006).

RNA isolation and qRT-PCR.

RNA was isolated using RNeasy Mini kit (QIAGEN). 1 µg RNA was reverse transcribed using Transcriptor First Strand cDNA kit (Roche) and oligo (dT) primers. Quantitative qRT-PCR analysis was performed as previously described (Yasmin et al., 2013). SYBR Green and CFX96 Real-Time PCR system (Bio-Rad) were used for quantitative real-time PCR. Cycling conditions for qRT-PCR were 3 min at 95°C, followed by 40 cycles of 30 sec at 95°C, 30 sec at 60°C, and 30 sec at 72°C. Following qRT-PCR primers were used; ALK2_F, 5′-TTGGAGACAGCACTTTAGCAG-3′; ALK2_R, 5′-GCGAGCCACTGTTCTTTGT-3′; ALK3_F, 5′-GAGTTGCTGCATTGCTGAC-3′; ALK3_R, 5′-GAGCCATGTAGCGTTTGGT-3′; ALK5_F, 5′-AGGCCAAATATCCCAAACAG-3′; ALK5_R, 5′-TAGCTGCTCCATTGGCATAC-3′; TGF-β1_F, 5′-GTACCTGAACCCGTGTTGCT-3′; TGF-β1_R, 5′-GTATCGCCAGGAATTGTTGC-3′; HPRT_F, 5′-GACCAGTCAACAGGGGACAT-3′; HPRT_R, 5′-AACACTTCGTGGGGTCCTTTTC-3′; TARC_F, 5′-CCATTCCCCTTAGAAAGCTG-3′; TARC_R, 5′-CTCTCAAGGCTTTGCAGGTA-3′. Results were analyzed using the delta delta Ct method and presented as fold difference in mRNA level relative to HPRT.

Retroviral vectors, transfection of packaging cell lines and gene transduction.

ALK2-HASLwt-IRES-GFP, ALK3-HASLwt-IRES-GFP and ALK5-HASLwt-IRES-GFP were obtained by cutting ALK2-HASLwt-pCDNA3, ALK3-HASLwt-pCDNA3 and ALK5-HASLwt-pCDNA3 (kind gift of Dr. Peter ten Dijke, LUMC, MCB Netherlands) with EcoRI and XhoI and inserting it into PBMN-IRES-GFP vector. Transfection of packaging cell line phoenix-GP as well as infection of target cells was done as previously described (Platzer et al., 2004). In brief, to produce recombinant amphotropic retrovirus, vectors were transiently transfected into the packaging cell line Phoenix-GP (Gag-Pol) using a calcium-phosphate protocol (https://www.stanford.edu/group/nolan/protocols/pro_helper_dep.html). Phoenix-GP was co-transfected with an expression plasmid encoding gibbon ape leukemia virus (GALV) envelope (gift from D. B. Kohn, Los Angeles, CA). Before gene transduction, fresh or thawed $CD34^+$ cells were stimulated overnight in X-VIVO 15 medium supplemented with the cytokines SCF (50 ng/mL), FLT3L (50 ng/mL), and TPO (50 ng/mL). Afterward, 1 mL retroviral supernatant (harvested 36 - 48 hours after transfection of packaging cells) was added to 4 x 10^4 $CD34^+$ HPCs in the presence of plate bound RetroNectin (Takara Bio, Shiga, Japan) using non-tissue culture-treated 24-well plates (Cellstar; Greiner Bio-One GmbH, Kremsmuenster, Austria) following the instructions of the manufacturer. Infections were repeated 2 to 3 times at intervals of 12 to 24 hours using fresh virus supernatants in the presence of cytokines SCF, FLT3L and TPO. Within

60 hours of the first transduction cycle, cells were harvested and re-cultured in LC, moDCs and monocyte/macrophage (Mϕ) lineage-conditions.

Immunofluorescence and Immunohistochemistry.

Prenatal and adult skin specimens were embedded in optimum cutting tissue compound (Tissue-Tek; Sakura), snap frozen in liquid nitrogen and stored at -80°C until further processing. Sections (6 μm) were cut, air dried, fixed in ice-cold acetone for 10 min, blocked with PBS 2% BSA for 1 hour at RT and stained with the primary unconjugated control rabbit isotype IgG (1:200; sc-3888; Santa Cruz Biotechnology) or antibodies specific for BMP4 (1:100; ab31165, abcam) or BMP7 (1:200; LS-B4567/39975; LifeSpan Biosciences) overnight at 4°C. The slides were washed with PBS and stained with the secondary goat anti-rabbit Alexa Fluor 546 (Invitrogen) for 2 hours at RT. Alexa Fluor 488 anti-Laminin5 (D4B5; Millipore) was used to visualize the dermo-epidermal junction. Nuclei were stained with DAPI. Pictures were taken using a LSM700 microscope and Zen 2009 software (Carl Zeiss, Vienna, Austria). For immunohistochemistry, human tissue sections were then incubated with anti-LAP (27232; R&D Systems) and anti–TGF-β1 serum (Santa Cruz Biotechnology, Inc.) overnight at 4°C, followed by biotin-conjugated goat anti–rabbit IgG for 2 h at room temperature using the Elite rabbit IgG Vectastain kits. Biotinylated antibodies were detected with HRP streptavidin and staining was visualized with amino-ethyl-carbazole (AEC; Dako). Finally, sections were mounted with Aquatex (Merck) and examined using a microscope (Eclipse 80; Nikon). Mouse epidermal sheets were prepared as described previously (Bauer et al., 2012). Epidermis was fixed in acetone for 10 – 20 min, blocked with PBS containing 2% BSA for 1 hour at RT and stained with Ab specific for I-A/I-E (PE-conjugated; 1:400; Biolegend) overnight at 4°C. The slides were washed with PBS and stained with DAPI to visualize the nuclei. Images from 7 randomly chosen microscopic fields were acquired. LCs were enumerated and mean values were calculated per ear sheet. Pictures were taken using a microscope (Eclipse 80i; Nikon) and Lucia G software (Laboratory Imaging).

RNA isolation, amplification and gene chip hybridization.

Total RNA from 3 independent donors was isolated from sorted cells by using RNeasy Micro Kit (QIAGEN) according to the manufacturer recommendations. Quality control with the RNA 6000 Pico LabChip Kit (Agilent, Cat.No. 5065-1513) on Agilent BioAnalyzer 2100 (Agilent, Foster City , CA) showed a RIN 9.9 - 10. cRNA target synthesis, amplification, hybridization to the GeneChip Human Genome U133 Plus 2.0 Array and scanning were done according to the standard protocols recommended by the manufacturer (Affymetrix, Santa Clara, CA). In brief,

cDNA was generated from 50 ng total RNA using T7-oligo(dT) promoter primer (Affymetrix GeneChip GeneChip® 3' IVT Express Kit, Cat.No. 901228). After a second strand cDNA synthesis, cDNA was converted to cRNA by an *in vitro* transcription reaction (Life Technologies). Thereafter, cRNA was purified and the yield was controlled with a spectrophotometer. Labelled cRNA was purified, quality controlled with Agilent 2100 Bioanalyzer and denatured at 94°C before hybriidization of 12 μg of the purified sample. The samples were hybridized to the Human Genome U133 Plus 2.0 Array at 45°C for 16 h (60 rpm) in an hybridization oven. The arrays were then processed on the Affymetrix Genechip® fluidics station 450: protocol FS450_0001 for Cartridge Arrays. They were washed, stained with streptavidin-PE (Affymetrix GeneChip® HT hybridization, Wash and Stain Kit (Cat No. 900720), washed again and scanned with a GeneArray Scanner (Affymetrix GCS3000).

Raw and normalized microarray experiments have been submitted to the Gene Expression Omnibus (GEO; accession number GSE49085). Fluorescent intensity was analyzed using the GeneChip Operating Software (GCOS) 1.1 (Affymetrix) and scaled to a target value of 100. Data uploaded into Expression Console EC1.2.1.20 (Affymetrix), normalized with the MAS5 algorithm and for log transformed data (Robust Multi-Array (RMA)) was used for the generation of CEL-files. The intensities below 200 were considered to be below positive expression and compared with signal intensities of previously published arrays (Lundberg et al., 2013) (MAS5 normalized data; Table SI). Transcripts differentially expressed among all samples were identified using ANOVA analysis within multiple testing cut off (false discovery rate (FDR) is 5%, significance level is 0.05). Relationship between different cell populations was demonstrated by the minimal spanning tree analysis. Additionally, hierarchical clustering was performed using Cluster 3.0, based on complete linkage and Euclidean distance measure and heat maps of selected genes (listed in Table SI) were subsequently produced using Java Treeview 1.0.12. Fold change of transcripts => 1.5 was considered as up regulation and vice versa. Fold change of important transcripts was compared with different subsets of LCs as described in Table SII.

Bmp7$^{\Delta/\Delta}$ mice and LacZ staining of tissues.

The generation of *Bmp7*$^{\Delta/\Delta}$ mice has previously been described (Zouvelou et al., 2009). All mouse lines were backcrossed for more than 8 generations into the C57Bl6/J background. Tissues from heterozygous *Bmp7lacZ* (*Bmp7*$^{wt/lacZ}$) mice (expressing β-galactosidase under the control of the *Bmp7* promoter) were stained with X-gal to identify the location of *Bmp7* expression. Briefly, isolated epidermal tissue was fixed in 2% formaldehyde, 0.2% glutaraldehyde, 0.01% sodium deoxycholate, 0.02% Nonidet-P40 (NP40) in PBS for 5 min,

washed with 2 mM $MgCl_2$ and stained at RT in the dark for several hours to overnight in X-gal staining solution, which contained 0.1 M phosphate pH 7.3, 2 mM $MgCl_2$, 0.01% sodium deoxycholate, 0.02% NP40, 5 mM $K_3[Fe(CN)_6]$, 5 mM $K_4[Fe(CN)_6]$ supplemented with 1 mg X-Gal (Promega)/ml. The samples were washed and refixed in 4% PFA and mounted with water-based Mowiol 4-88 (Sigma) and documented using a Leica DM-E microscope equipped with a Leica DFC290 camera. Experimental results were obtained from at least three independent samples. Mice were maintained at the animal facilities of the University of Zurich. Animal experiments were approved by the local veterinary authorities (permit 98/2011, Veterinäramt Zürich) in compliance with Swiss federal law (TSchG, TSchV) and cantonal by-laws in full compliance with the European Guideline 86/609/EC. This authority approval also included ethical approval.

Western blot analysis.

Cells were directly lysed in 13 SDS-loading dye at 95 □C for 5 min. For Western blot analysis, lysates of 1 - $2x10^5$ cells per lane were loaded on 10 % SDS-polyacrylamide gels. Resolved proteins were transferred to a polyvinylene-difluoride membrane (Immobilon-P; Millipore, Billerica, MA) as previously described (Yasmin et al., 2013). Membranes were probed with antibodies against rabbit-pSmad1 (Ser463/465)/Smad5 (Ser463/465)/Smad8 (Ser426/428), rabbit-pSmad2 (Ser465/467) and rabbit-pSmad3 (Ser423/425) (Cell Signaling Technology), rabbit-Smad1/5/8 (N-18)-R: sc-6031-R and goat-Smad2/3 (E-20): sc-6033 (Santa Cruz) followed by horseradish peroxidase (HRP)-conjugated goat anti-rabbit, rabbit anti-goat (Pierce Biotechnology, Rockford, IL). Detection was performed with the chemiluminescent substrate SuperSignal WestPico or WestDura (Pierce Biotechnology).

Flow cytometry.

Flow cytometry staining and analysis were performed as described previously (Yasmin et al., 2013). Murine monoclonal antibodies (mAbs) of the following specificities were used: FITC-conjugated mAb specific for CD1a, phycoerythrin (PE)-conjugated mAb specific for CD207 (Immunotech, Marseille, France), allophycocyanin-conjugated antibody for CD324, pacific blue conjugated CD1a and CD14 (APC-CY7) (BioLegend, San Diego, CA), CD11b (PE-CY7; BD Bioscience) and MPO-C2 (PE; ADG ANDER GRUB, Austria). All stainings were done with permeabilized cells. Flow cytometric analysis was performed using an LSRII instrument (BD) and FlowJo software (Tree Star).

T cell proliferation assays.

T cell proliferation assay (MLR) was performed as described before (Stockl et al., 1999). Briefly, purified LC clusters were seeded ($5x10^4$ to $1x10^5$/500ul) in 48-well plate and activated with PGN. Graded numbers of these stimulator cells were co-cultured with a constant number of 5×10^4 to 1×10^5 highly purified (> 98 %) allogeneic T cells in RPMI medium containing 10 % FCS using round-bottom, 96-well tissue culture plates (Nalge Europe, Brussels, Belgium). Proliferation of T cells was monitored on day 5 of culture by adding [methyl-^{3}H]TdR followed by measuring [methyl-^{3}H]TdR incorporation 18 hours later. Incorporated radioactivity was measured using a 1450 microbeta plate reader (Wallac-Trilux Instrument; Life Science, Vienna, Austria). The basal proliferation rate of T cell control was 900 ± 200 cell counts. Supernatents were collected for cytokine measurement before adding [methyl-^{3}H]TdR. Assays were performed in triplicates.

Cytokine measurement.

Purified LC clusters were seeded ($5x10^4$ to $1x10^5$/500µl) in 48-well plate. Cells were activated with PGN and supernatants were collected 48 hours later as described previously (Jurkin et al., 2010). Quantification of cytokines produced by LCs or LC:T cell co-cultures was performed using the Luminex system (Austin, TX).

Statistical analysis.

Statistical analysis was performed using the paired, 2-tailed Student t test or ANOVA; p-values of less than 0.05 were considered significant.

Disclosure of conflict of Interest.

The authors have no conflict of interest.

Acknowledgements.

G. Zlabinger, M. Merio and P. Waidhofer-Söllner are acknowledged for performing cytokine measurements. This work was supported by a PhD fellowship of the High Education Commission of Pakistan to N. Y., by grants from the Austrian Science Fund (FWF, P22058, P19245, P25720, SFB-2304 to H. S., P23215-B11 to R. K., PhD program W1212 "Inflammation and Immunity" to T. B. and FWF grant P19474-B13 to A.E.-B.

REFERENCES

Bascom, C.C., J.R. Wolfshohl, R.J. Coffey, Jr., L. Madisen, N.R. Webb, A.R. Purchio, R. Derynck, and H.L. Moses. 1989. Complex regulation of transforming growth factor beta 1, beta 2, and beta 3 mRNA expression in mouse fibroblasts and keratinocytes by transforming growth factors beta 1 and beta 2. *Mol Cell Biol* 9:5508-5515.

Bauer, T., A. Zagorska, J. Jurkin, N. Yasmin, R. Köffel, S. Richter, B. Gesslbauer, G. Lemke, and H. Strobl. 2012. Identification of Axl as a downstream effector of TGF-beta1 during Langerhans cell differentiation and epidermal homeostasis. *J Exp Med* 209:2033-2047.

Bitgood, M.J., and A.P. McMahon. 1995. Hedgehog and Bmp genes are coexpressed at many diverse sites of cell-cell interaction in the mouse embryo. *Dev Biol* 172:126-138.

Bobr, A., B.Z. Igyarto, K.M. Haley, M.O. Li, R.A. Flavell, and D.H. Kaplan. 2012. Autocrine/paracrine TGF-beta1 inhibits Langerhans cell migration. *Proc Natl Acad Sci U S A* 109:10492-10497.

Borkowski, T.A., J.J. Letterio, A.G. Farr, and M.C. Udey. 1996. A role for endogenous transforming growth factor beta 1 in Langerhans cell biology: the skin of transforming growth factor beta 1 null mice is devoid of epidermal Langerhans cells. *J Exp Med* 184:2417-2422.

Botchkarev, V.A. 2003. Bone morphogenetic proteins and their antagonists in skin and hair follicle biology. *J Invest Dermatol* 120:36-47.

Botchkarev, V.A., N.V. Botchkareva, W. Roth, M. Nakamura, L.H. Chen, W. Herzog, G. Lindner, J.A. McMahon, C. Peters, R. Lauster, A.P. McMahon, and R. Paus. 1999. Noggin is a mesenchymally derived stimulator of hair-follicle induction. *Nat Cell Biol* 1:158-164.

Caux, C., C. Dezutter-Dambuyant, D. Schmitt, and J. Banchereau. 1992. GM-CSF and TNF-alpha cooperate in the generation of dendritic Langerhans cells. *Nature* 360:258-261.

Caux, C., C. Massacrier, B. Dubois, J. Valladeau, C. Dezutter-Dambuyant, I. Durand, D. Schmitt, and S. Saeland. 1999. Respective involvement of TGF-beta and IL-4 in the development of Langerhans cells and non-Langerhans dendritic cells from CD34+ progenitors. *J Leukoc Biol* 66:781-791.

Chang-Rodriguez, S., W. Hoetzenecker, C. Schwarzler, T. Biedermann, S. Saeland, and A. Elbe-Burger. 2005. Fetal and neonatal murine skin harbors Langerhans cell precursors. *J Leukoc Biol* 77:352-360.

Chorro, L., A. Sarde, M. Li, K.J. Woollard, P. Chambon, B. Malissen, A. Kissenpfennig, J.B. Barbaroux, R. Groves, and F. Geissmann. 2009. Langerhans cell (LC) proliferation mediates neonatal development, homeostasis, and inflammation-associated expansion of the epidermal LC network. *J Exp Med* 206:3089-3100.

Daly, A.C., R.A. Randall, and C.S. Hill. 2008. Transforming growth factor beta-induced Smad1/5 phosphorylation in epithelial cells is mediated by novel receptor complexes and is essential for anchorage-independent growth. *Mol Cell Biol* 28:6889-6902.

Dennler, S., M.J. Goumans, and P. ten Dijke. 2002. Transforming growth factor beta signal transduction. *J Leukoc Biol* 71:731-740.

Ebner, R., R.H. Chen, S. Lawler, T. Zioncheck, and R. Derynck. 1993. Determination of type I receptor specificity by the type II receptors for TGF-beta or activin. *Science* 262:900-902.

Elbe, A., E. Tschachler, G. Steiner, A. Binder, K. Wolff, and G. Stingl. 1989. Maturational steps of bone marrow-derived dendritic murine epidermal cells. Phenotypic and functional studies on Langerhans cells and Thy-1+ dendritic epidermal cells in the perinatal period. *J Immunol* 143:2431-2438.

Fainaru, O., E. Woolf, J. Lotem, M. Yarmus, O. Brenner, D. Goldenberg, V. Negreanu, Y. Bernstein, D. Levanon, S. Jung, and Y. Groner. 2004. Runx3 regulates mouse TGF-beta-mediated dendritic cell function and its absence results in airway inflammation. *EMBO J* 23:969-979.

Feng, X.H., and R. Derynck. 2005. Specificity and versatility in tgf-beta signaling through Smads. *Annu Rev Cell Dev Biol* 21:659-693.

Gatti, E., M.A. Velleca, B.C. Biedermann, W. Ma, J. Unternaehrer, M.W. Ebersold, R. Medzhitov, J.S. Pober, and I. Mellman. 2000. Large-scale culture and selective maturation of human Langerhans cells from granulocyte colony-stimulating factor-mobilized CD34+ progenitors. *J Immunol* 164:3600-3607.

Geissmann, F., C. Prost, J.P. Monnet, M. Dy, N. Brousse, and O. Hermine. 1998. Transforming growth factor beta1, in the presence of granulocyte/macrophage colony-stimulating factor and interleukin 4, induces differentiation of human peripheral blood monocytes into dendritic Langerhans cells. *J Exp Med* 187:961-966.

Geissmann, F., P. Revy, A. Regnault, Y. Lepelletier, M. Dy, N. Brousse, S. Amigorena, O. Hermine, and A. Durandy. 1999. TGF-beta 1 prevents the noncognate maturation of human dendritic Langerhans cells. *J Immunol* 162:4567-4575.

Goumans, M.J., G. Valdimarsdottir, S. Itoh, A. Rosendahl, P. Sideras, and P. ten Dijke. 2002. Balancing the activation state of the endothelium via two distinct TGF-beta type I receptors. *EMBO J* 21:1743-1753.

Gupta, A.K., C. Rusterholz, W. Holzgreve, and S. Hahn. 2005. Constant IFNgamma mRNA to protein ratios in cord and adult blood T cells suggests regulation of IFNgamma expression in cord blood T cells occurs at the transcriptional level. *Clin Exp Immunol* 140:282-288.

Hacker, C., R.D. Kirsch, X.S. Ju, T. Hieronymus, T.C. Gust, C. Kuhl, T. Jorgas, S.M. Kurz, S. Rose-John, Y. Yokota, and M. Zenke. 2003. Transcriptional profiling identifies Id2 function in dendritic cell development. *Nat Immunol* 4:380-386.

Heinz, L.X., B. Platzer, P.M. Reisner, A. Jörgl, S. Taschner, F. Göbel, and H. Strobl. 2006. Differential involvement of PU.1 and Id2 downstream of TGF-beta1 during Langerhans-cell commitment. *Blood* 107:1445-1453.

Helder, M.N., E. Ozkaynak, K.T. Sampath, F.P. Luyten, V. Latin, H. Oppermann, and S. Vukicevic. 1995. Expression pattern of osteogenic protein-1 (bone morphogenetic protein-7) in human and mouse development. *J Histochem Cytochem* 43:1035-1044.

Hoshino, N., N. Katayama, T. Shibasaki, K. Ohishi, J. Nishioka, M. Masuya, Y. Miyahara, M. Hayashida, D. Shimomura, T. Kato, K. Nakatani, K. Nishii, K. Kuribayashi, T. Nobori, and H. Shiku. 2005. A novel role for Notch ligand Delta-1 as a regulator of human Langerhans cell development from blood monocytes. *J Leukoc Biol* 78:921-929.

Hutter, C., M. Kauer, I. Simonitsch-Klupp, G. Jug, R. Schwentner, J. Leitner, P. Bock, P. Steinberger, W. Bauer, N. Carlesso, M. Minkov, H. Gadner, G. Stingl, H. Kovar, and E. Kriehuber. 2012. Notch is active in Langerhans cell histiocytosis and confers pathognomonic features on dendritic cells. *Blood* 120:5199-5208.

Hwang, E.A., H.B. Lee, and K.C. Tark. 2001. Comparison of bone morphogenetic protein receptors expression in the fetal and adult skin. *Yonsei Med J* 42:581-586.

Igyarto, B.Z., and D.H. Kaplan. 2012. Antigen presentation by Langerhans cells. *Curr Opin Immunol*

Izumi, N., S. Mizuguchi, Y. Inagaki, S. Saika, N. Kawada, Y. Nakajima, K. Inoue, S. Suehiro, S.L. Friedman, and K. Ikeda. 2006. BMP-7 opposes TGF-beta1-mediated collagen induction in mouse pulmonary myofibroblasts through Id2. *Am J Physiol Lung Cell Mol Physiol* 290:L120-126.

Jurkin, J., Y.M. Schichl, R. Köffel, T. Bauer, S. Richter, S. Konradi, B. Gesslbauer, and H. Strobl. 2010. miR-146a is differentially expressed by myeloid dendritic cell subsets and desensitizes cells to TLR2-dependent activation. *J Immunol* 184:4955-4965.

Kane, C.J., A.M. Knapp, J.N. Mansbridge, and P.C. Hanawalt. 1990. Transforming growth factor-beta 1 localization in normal and psoriatic epidermal keratinocytes in situ. *J Cell Physiol* 144:144-150.

Kaplan, D.H., M.O. Li, M.C. Jenison, W.D. Shlomchik, R.A. Flavell, and M.J. Shlomchik. 2007. Autocrine/paracrine TGFbeta1 is required for the development of epidermal Langerhans cells. *J Exp Med* 204:2545-2552.

Kel, J.M., M.J. Girard-Madoux, B. Reizis, and B.E. Clausen. 2010. TGF-beta is required to maintain the pool of immature Langerhans cells in the epidermis. *J Immunol* 185:3248-3255.

Keski-Oja, J., and K. Koli. 1992. Enhanced production of plasminogen activator activity in human and murine keratinocytes by transforming growth factor-beta 1. *J Invest Dermatol* 99:193-200.

Krystal, G., V. Lam, W. Dragowska, C. Takahashi, J. Appel, A. Gontier, A. Jenkins, H. Lam, L. Quon, and P. Lansdorp. 1994. Transforming growth factor beta 1 is an inducer of erythroid differentiation. *J Exp Med* 180:851-860.

Li, A.G., S.L. Lu, G. Han, K.E. Hoot, and X.J. Wang. 2006. Role of TGFbeta in skin inflammation and carcinogenesis. *Mol Carcinog* 45:389-396.

Lundberg, K., A.S. Albrekt, I. Nelissen, S. Santegoets, T.D. de Gruijl, S. Gibbs, and M. Lindstedt. 2013. Transcriptional profiling of human dendritic cell populations and models--unique profiles of in vitro dendritic cells and implications on functionality and applicability. *PLoS One* 8:e52875.

Lyons, K.M., R.W. Pelton, and B.L. Hogan. 1989. Patterns of expression of murine Vgr-1 and BMP-2a RNA suggest that transforming growth factor-beta-like genes coordinately regulate aspects of embryonic development. *Genes Dev* 3:1657-1668.

Massague, J. 1998. TGF-beta signal transduction. *Annu Rev Biochem* 67:753-791.

Merad, M., M.G. Manz, H. Karsunky, A. Wagers, W. Peters, I. Charo, I.L. Weissman, J.G. Cyster, and E.G. Engleman. 2002. Langerhans cells renew in the skin throughout life under steady-state conditions. *Nat Immunol* 3:1135-1141.

Miyazono, K., Y. Kamiya, and M. Morikawa. 2010. Bone morphogenetic protein receptors and signal transduction. *J Biochem* 147:35-51.

Oh, S.P., T. Seki, K.A. Goss, T. Imamura, Y. Yi, P.K. Donahoe, L. Li, K. Miyazono, P. ten Dijke, S. Kim, and E. Li. 2000. Activin receptor-like kinase 1 modulates transforming growth factor-beta 1 signaling in the regulation of angiogenesis. *Proc Natl Acad Sci U S A* 97:2626-2631.

Platzer, B., A. Jörgl, S. Taschner, B. Hocher, and H. Strobl. 2004. RelB regulates human dendritic cell subset development by promoting monocyte intermediates. *Blood* 104:3655-3663.

Romani, N., P.M. Brunner, and G. Stingl. 2012. Changing views of the role of Langerhans cells. *J Invest Dermatol* 132:872-881.

Romani, N., G. Schuler, and P. Fritsch. 1986. Ontogeny of Ia-positive and Thy-1-positive leukocytes of murine epidermis. *J Invest Dermatol* 86:129-133.

Schmierer, B., and C.S. Hill. 2007. TGFbeta-SMAD signal transduction: molecular specificity and functional flexibility. *Nat Rev Mol Cell Biol* 8:970-982.

Schuster, C., C. Vaculik, C. Fiala, S. Meindl, O. Brandt, M. Imhof, G. Stingl, W. Eppel, and A. Elbe-Bürger. 2009. HLA-DR+ leukocytes acquire CD1 antigens in embryonic and fetal human skin and contain functional antigen-presenting cells. *J Exp Med* 206:169-181.

Stöckl, J., H. Vetr, O. Majdic, G. Zlabinger, E. Kuechler, and W. Knapp. 1999. Human major group rhinoviruses downmodulate the accessory function of monocytes by inducing IL-10. *J Clin Invest* 104:957-965.

Stoitzner, P., H. Stossel, M. Wankell, S. Hofer, C. Heufler, S. Werner, and N. Romani. 2005. Langerhans cells are strongly reduced in the skin of transgenic mice overexpressing follistatin in the epidermis. *Eur J Cell Biol* 84:733-741.

Strobl, H., C. Bello-Fernandez, E. Riedl, W.F. Pickl, O. Majdic, S.D. Lyman, and W. Knapp. 1997. flt3 ligand in cooperation with transforming growth factor-beta1 potentiates in

vitro development of Langerhans-type dendritic cells and allows single-cell dendritic cell cluster formation under serum-free conditions. *Blood* 90:1425-1434.

Strobl, H., E. Riedl, C. Scheinecker, C. Bello-Fernandez, W.F. Pickl, K. Rappersberger, O. Majdic, and W. Knapp. 1996. TGF-beta 1 promotes in vitro development of dendritic cells from CD34+ hemopoietic progenitors. *J Immunol* 157:1499-1507.

Takahashi, H., and T. Ikeda. 1996. Transcripts for two members of the transforming growth factor-beta superfamily BMP-3 and BMP-7 are expressed in developing rat embryos. *Dev Dyn* 207:439-449.

Taschner, S., C. Koesters, B. Platzer, A. Jörgl, W. Ellmeier, T. Benesch, and H. Strobl. 2007. Down-regulation of RXRalpha expression is essential for neutrophil development from granulocyte/monocyte progenitors. *Blood* 109:971-979.

Yasmin, N., S. Konradi, G. Eisenwort, Y.M. Schichl, M. Seyerl, T. Bauer, J. Stöckl, and H. Strobl. 2013. beta-Catenin Promotes the Differentiation of Epidermal Langerhans Dendritic Cells. *J Invest Dermatol* 133:1250-1259.

Ying-Ping Xu, Y.S., Zhi-Zhong Cui, Hong H Jiang, Li Li, Xiao-Fan Wang, Li Zhou and Qing-Sheng Mi. 2012. TGFβ/Smad3 Signal Pathway Is Not Required for Epidermal Langerhans Cell Development. *Journal of investigative dermatology* 2106-2109.

Young, J.W., P. Szabolcs, and M.A. Moore. 1995. Identification of dendritic cell colony-forming units among normal human CD34+ bone marrow progenitors that are expanded by c-kit-ligand and yield pure dendritic cell colonies in the presence of granulocyte/macrophage colony-stimulating factor and tumor necrosis factor alpha. *J Exp Med* 182:1111-1119.

Zahner, S.P., J.M. Kel, C.A. Martina, I. Brouwers-Haspels, M.A. van Roon, and B.E. Clausen. 2011. Conditional Deletion of TGF-betaR1 Using Langerin-Cre Mice Results in Langerhans Cell Deficiency and Reduced Contact Hypersensitivity. *J Immunol* 187:5069-5076.

Zouvelou, V., O. Passa, K. Segklia, S. Tsalavos, D.M. Valenzuela, A.N. Economides, and D. Graf. 2009. Generation and functional characterization of mice with a conditional BMP7 allele. *Int J Dev Biol* 53:597-603.

FIGURE LEGENDS

Figure 1. TGF-β1 induces LC differentiation through type-I receptor ALK3.

(A) Pre-expanded $CD34^+$ cells were treated or not with ALK4/5/7 inhibitor (SB421543) or ALK2/3/6 inhibitor (dorsomorphin) for 1 h before TGF-β1 addition. FACS plots represent day 3-generated LCs in the presence or absence of inhibitors analyzed for $CD1a^+CD207^+$ by flow cytometry. Data are representative of six independent experiments. Bar diagrams represent percentages and total numbers of cells expressing $CD1a^+CD207^+$, $CD1a^+$, $CD11b^+$ or $CD14^+$ cells (± SEM, *P < 0.05, **P < 0.004). **(B)** Day 7-generated LCs were incubated in the presence or absence of SB421543 and analyzed for CD1a and D207 by flow cytometry. Data are representative of three independent experiments. Graph represents total numbers of $CD1a^+CD207^+$ cells. **(C)** $CD34^+$ cells were transduced with retroviral vectors encoding ALK2-, ALK3- or ALK5- IRES-GFP and were cultured in the presence of TGF-β1**.** FACS plots represent day 7-generated GFP^+ cells analyzed for CD1a and CD207. Data are representative of three independent experiments. Bar diagram represent percentages of $CD1a^+CD207^+$ cells (± SEM, *P < 0.05). **(D)** $CD34^+$ cells were transduced with retroviral vector encoding ALK3-IRES-GFP and cultured in LC, moDCs and monocyte/macrophages (Mϕ) lineage-conditions. FACS plot represent day 7-generated GFP^+ cells analyzed for CD1a, CD207, CD11b, CD14 and MPO. Bar diagrams represent percentages of $CD1a^+$, $CD207^+$, $CD11b^+$, $CD14^+$ and MPO^+ cells. Data are representative of four independent experiments (± SEM, *P < 0.05).

Figure 2. BMP7 expression is detectable in the basal epidermis during human prenatal development.

(A) Skin sections (6 μm) from prenatal and adult human skin were analyzed for the expression of BMP7 (red) or control. Nuclei and the dermo-epidermal junction were visualized with Dapi (blue) and mAb directed against Laminin 5 (green) respectively. Data are representative of three donors for 8 – 10 weeks EGA, two donors for 11 – 14 weeks EGA and three donors for healthy adult skin. Bars 50 μm. **(B)** Immunofluorescence staining of BMP7 and HLA-DR at 8 wk EGA and adult human skin. Immunohistochemical staining was performed on cryostat sections. TGF-β1 was visualized with AEC (red). Data are representative of two independent experiments. Bars 50 μm.

Figure 3. LC impairment in Bmp7 deficient mice.

(A) Tissues from heterozygous *Bmp7lacZ* (*Bmp7*$^{wt/lacZ}$) mice (expressing β-galactosidase under the control of the *Bmp7* promoter) were stained with X-gal to identify the location of *Bmp7* expression. The Transcriptional activity of Bmp7 is revealed by lacZ staining in the epidermis of BMP7-lacZ mice. One representative image from 3 different mice and experiments is shown. **(B)** I-A/I-E–positive cells from the epidermis of WT and Bmp7-KO mice at birth (postnatal day 0 P0) were enumerated and shown in I-A/I-E$^+$ cells/mm^2. Graph shows the number of I-A/I-E$^+$ cells with each connected white and black dot, represents mean data from one independent litter. Bars indicate the mean ± SEM, *P < 0.05. **(C)** Representative immunofluorescence staining of an epidermal sheet from a WT and a BMP7-KO mouse. LCs were visualized with Abs against I-A/I-E (red) and nuclei were stained with DAPI (blue). Data are representative of four independent experiments. Insets represent higher magnification of framed areas. Bar: 50μm.

Figure 4. BMP7 induce LC differentiation.

(A) CD34$^+$ cells were incubated with GM-CSF, FLT3L, SCF and TNF in the presence of TGF-β1, BMP7 or control and morphology was assessed. FACS plots represent day 7-generated cells analyzed for the expression of CD1a, CD207 and E-cadherin. Bar diagrams represent percentages and total numbers of phenotypically defined cells generated as indicated. Data are representative of three independent experiments (*P < 0.05, **P < 0.005). **(B-C)** Cells were labeled with CFSE at day 4. CD1a$^+$ cells (left, data are representative of four independent experiments) and CD207$^+$ cells (right, data are representative of three independent experiments) were analyzed at day 6 by flow cytometry.

Figure 5. Activation of Smad1/5/8 drives LC differentiation.

(A) Pre-expanded CD34$^+$ cells were treated with TGF-β1 or BMP7 for the indicated times. Levels of immunoblot pSmad2/3, Smad2/3, pSmad1/5/8 and Smad1/5/8 were analyzed. Data are representative of five independent experiments. **(B)** LCs were generated in the presence of TGF-β1 or BMP7 and expression of ALK2, 3 and 5 was assessed during LC differentiation by qRT-PCR. Values were normalized to HPRT. Data are representative of three independent experiments (± SD, *P < 0.05). **(C)** TGF-β1 expression during LC differentiation was assessed by qRT-PCR. Data are representative of three independent experiments (± SD).

Figure 6. Higher pro-inflammatory cytokine production by BMP7-generated microbial stimulated LCs.

(A) Expanded $CD34^+$ cells were induced to differentiate into LCs in response to TGF-β1 or BMP7 stimulation as in 4A. LC clusters were purified using 1 g sedimentation, and CD1a and CD207 expression were analyzed by flow cytometry. Data are representative of four independent experiments. **(B)** Cluster purified LCs (TGF-β1 or BMP7) were activated or not with peptidoglycan (PGN) or Pam3CSK4 for 2 days and CD80 and CD86 expression was analyzed by flow cytometry. Data are representative of four independent experiments. **(C)** Cluster purified LCs (TGF-β1 or BMP7) were activated or not with peptidoglycan (PGN) for 2 days and supernatants were collected for cytokine measurement. Bar diagrams represent amounts of cytokines produced. Data are representative of four independent experiments (± SD, *$P < 0.05$, **$P < 0.005$). **(D)** T cells ($1x10^5$) were stimulated with indicated numbers of LCs. Proliferation of T cells was monitored on day 5 of culture by adding [methyl-^{3}H]TdR followed by measuring [methyl-^{3}H]TdR incorporation 18 h later. Error bars represent standard error mean of triplicate values. Data are representative of fourteen independent experiments (CB; cord blood, PB; peripheral blood). **(E)** TGF-β1- or BMP7-generated LCs were stimulated with PGN for 2 days and TARC expression was analyzed by qRT-PCR. Data are representative of four independent experiments (± SEM). **(F)** Allogeneic T cells were co-cultured with activated TGF-β1- or BMP7-LCs and production of IFNγ, IL-13 and IL-5 was measured by using the Luminex system (Austin, TX). Data are representative of four independent experiments (± SEM, CB; cord blood, PB; peripheral blood).

Figure 7. Gene expression analysis.

Clustering using complete linkage algorithm on differentially expressed transcripts, identified by ANOVA analysis within multiple testing cut off (false discovery rate (FDR) is 5%, significance level is 0.05), demonstrates relationship among *in vitro* and *ex vivo* LCs. Heat map visualizing gene expression profiles of differentially expressed genes (listed in Table SI) upon hierarchical clustering with complete linkage and euclidean measure. Colors represent high (red) and low (blue) normalized intensity. $CD1a^+CD207^+$ cells were generated from three independent donors (A, B, C) in response to TGF-β1 or BMP7 and were flow sorted prior to analysis.

Figure 8. Sequential addition of TGF-β1 to the BMP7-supplemented cultures enhances LC generation with minimal cytokine combination.

(A) $CD34^+$ cells were induced to differentiate into LCs in response to TGF-β1 or BMP7 for 7 days. Parallel cultures contained BMP7 for 5 days followed by TGF-β1 for the final 48 h

(BMP7+ TGF-β1, right). Control cultures did not contain any exogenous TGF-β1 or BMP7 (left). All the cultures were supplemented with GM-CSF, TNF, SCF and FLT3L. FACS plots represent day 7-generated cells analyzed for the expression of CD1a and CD207. Bar diagrams represent total numbers of $CD1a^+CD207^+$ cells observed in four independent experiments (± SD, *P < 0.05, **P < 0.005, **P < 0.0005). **(B)** LCs were generated in the presence of BMP7 for 6 days followed by late TGF-β1 addition (48 h). In the first culture phase (d 1 – d 6), different cytokine combinations were tested. FACS plots represent day 7-generated cells analyzed for the expression of CD1a and CD207. Bar diagrams represent mean total numbers of $CD1a^+CD207^+$ cells (± SEM) observed in three independent experiments. Graph represents different cytokine combinations used during LC differentiation as designated by a, b, c, d, e (statistically significant: a vs b; a vs e; b vs e, *P < 0.05). **(C)** LCs were generated in the presence of TGF-β1 for 7 days. Parallel cultures contained BMP7 for 5 days followed by late addition of TGF-β1 (48 h; BMP7+TGF-β1). All the cultures were supplemented with GM-CSF, TNF, SCF and FLT3L. LCs were cluster purified and activated or not with PGN for 48 h. Supernatants were collected for cytokine measurement. Bar diagrams represent mean amounts of cytokines produced in four independent experiments.

SUPPLEMENTARY INFORMATION

Table SI. Comparison of expression levels of important transcripts in LCs.

Yasmin et al.				(Lundberg et al., 2013)	
Probe Set ID	**Gene Symbol**	***in vitro* CD34-LCs (BMP7)**	***in vitro* CD34-LCs (TGF-β1)**	***in vitro* CD34-LCs**	***ex vivo* LCs**
204438_at	CD206/MRC1	+++	-	+++	-
220428_at	CD207/Langerin	+++	+++	+++	+++
207277_at	CD209/DC-SIGN	-	-	++	-
203799_at	CD302/DCL-1	+++	+++	++	+++
206682_at	CLEC10A	+++	+++	+++	+
211709_s_at	CLEC11A	++	+	+	-
221698_s_at	CLEC7A/Dectin1	+++	+++	+++	+++
211734_s_at	FCER1A	+++	+++	+	+++
204232_at	FCER1G	+++	+++	++	+++
203561_at	FCGR2A	+++	+	-	+
210889_s_at	FCGR2B	+++	++	-	++
211395_x_at	FCGR2C	+++	++	-	++
218831_s_at	FCGRT	+++	+++	+	++
37408_at	MRC2	+++	+++	++	-
224983_at	SCARB2	++	++	+	+
206995_x_at	SCARF1	+++	+++	-	+
210176_at	TLR1	+++	+++	+	-
204924_at	TLR2	+++	+	+	-
Interleukins and their receptors					
206295_at	IL18	+++	+++	+	+
219323_s_at	IL18BP	-	-	-	++
39402_at	IL1B	+++	++	++	+++
212659_s_at	IL1RN	+++	++	+	-
202859_x_at	IL8	++	-	-	+
204912_at	IL10RA	+++	+++	+++	+++
209575_at	IL10RB	+++	+++	+	-
201887_at	IL13RA1	+++	+++	+++	+++
229101_at	IL17RA	+++	++	+	-
219255_x_at	IL17RB	-	-	+	-
202948_at	IL1R1	+++	+++	+++	+++
205403_at	IL1R2	+++	+++	+++	+++
205227_at	IL1RAP	+++	+++	+++	++
242809_at	IL1RL1	-	-	+	-
237493_at	IL22RA2	+++	+++	+	-

205926_at	IL27RA	++	++	+	+
203233_at	IL4R	+++	+++	+	+
205945_at	IL6R	+++	+++	++	++
212195_at	IL6ST	+++	+++	+++	+++
226218_at	IL7R	+++	+++	++	+
Signaling Molecules					
209906_at	C3AR1	+++	++	+	-
211287_x_at	CSF2RA	+++	++	+	-
205159_at	CSF2RB	+++	+++	+++	+++
225661_at	IFNAR1	++	++	+	-
211676_s_at	IFNGR1	+++	+++	-	+
201642_at	IFNGR2	+++	+++	++	++
201105_at	LGALS1	+++	+++	+++	+++
208949_s_at	LGALS3	+++	+++	+++	+++
208934_s_at	LGALS8	++	++	+	+
206631_at	PTGER2	-	-	+	-
204897_at	PTGER4	+++	+++	+++	+++
224937_at	PTGFRN	+++	+++	+	-
1552807_a_at	SIGLEC10	+++	+++	+++	+++
207113_s_at	TNF	+++	+++	-	++
209295_at	TNFRSF10B	+++	+++	++	+
227345_at	TNFRSF10D	+	+	+	-
207037_at	TNFRSF11A	+	+	+	-
209354_at	TNFRSF14	++	++	+	+
207643_s_at	TNFRSF1A	+++	+++	+	+
203508_at	TNFRSF1B	+++	++	-	+
210314_x_at	TNFSF13	+++	+++	++	+
CD antigens					
205055_at	CD103	+++	+++	++	+
226545_at	CD109	+++	+++	++	++
207315_at	CD226	-	-	+	-
216379_x_at	CD24	-	-	++	-
1559583_at	CD276	-	-	+	-
217078_s_at	CD300A	+++	+	-	+
209555_s_at	CD36	+++	++	+++	-
216424_at	CD4	-	-	-	+++
217523_at	CD44	++	++	+++	+++
208783_s_at	CD46	+++	+++	+++	+++
242974_at	CD47	++	++	++	+++
204118_at	CD48	+++	+++	+	-
34210_at	CD52	+++	+++	++	+++

203416_at	CD53	+++	+++	+++	+++
1555950_a_at	CD55	+++	+++	+	+++
205173_x_at	CD58	+++	+++	++	+++
200985_s_at	CD59	+++	+++	++	++
200663_at	CD63	+++	+++	+++	+++
209795_at	CD69	+++	++	++	+++
207332_s_at	CD71	+++	+++	+++	+++
209619_at	CD74	+++	+++	+++	+++
1555779_a_at	CD79A	-	-	++	++
230391_at	CD84	+++	+++	+	+
233317_at	CD9	-	-	++	+++
202877_s_at	CD93	-	-	++	-
Chemokines and receptors					
216714_at	CCL13	-	-	++	-
207900_at	CCL17	++	+	+	-
207861_at	CCL22	+++	+++	+++	+++
204103_at	CCL4	-	-	-	++
205099_s_at	CCR1	-	-	+++	-
206978_at	CCR2	+	-	+++	-
206991_s_at	CCR5	++	-	+	-
206337_at	CCR7	+	+	+	-
219161_s_at	CKLF	+++	+++	+++	+++
205898_at	CX3CR1	+++	+++	-	+++
223454_at	CXCL16	++	-	+	+++
211919_s_at	CXCR4	+++	+	+++	++
Maturation/Presentation					
35150_at	CD40	++	++	+	+
200675_at	CD81	+++	+++	+++	++
204440_at	CD83	+++	+++	+++	+++
210895_s_at	CD86	+++	+++	+	+++
206749_at	CD1B	+++	+++	+++	+
205987_at	CD1C	+++	+++	+++	+++
210325_at	CD1A	+++	+++	+++	+++
215784_at	CD1E	+++	+++	+++	+++
205569_at	CD208/LAMP3	+++	+++	+++	+++
Adhesion					
208654_s_at	CD164	+++	+++	++	++
206120_at	CD33	+++	+++	+	-
205884_at	CD49D	++	-	++	-
202910_s_at	CD97	+++	+++	-	++
202637_s_at	ICAM1	+++	+++	+	+

204949_at	ICAM3	+++	+++	+++	+++
209879_at	SELPLG	+++	+++	+	+
216537_s_at	SIGLEC7	-	-	+	-
Others					
224629_at	LMAN1	+++	+++	+++	++
200805_at	LMAN2	+++	+++	++	+
200900_s_at	M6PR	+++	+++	+++	++

--Expression levels of transcripts encoding TLRs, CD antigens, lectins, TNF molecules, chemokines, interleukins and receptors, selected based on positive expression in the *in vitro* LCs.

--Signal intensity levels (MAS5 based): - :< 200; + : 200-500; ++ : 500-1000; +++ :>1000.

--LC - Langerhans Cell; CD34-LC - *in vitro* derived Langerhans Cell from $CD34^+$ precursor.

Table SII. Comparison of fold change of important transcripts in LCs.

Probe Set ID	Gene Symbol	*in vitro* CD34-LCs (BMP7) vs CD34-LCs (TGF-β1)	*in vitro* CD34-LCs (BMP7) vs CD34-LCs (Lundberg et al., 2013)	*in vitro* CD34-LCs (TGF-β1) vs CD34-LCs (Lundberg et al., 2013)	*in vitro* CD34-LCs (BMP7) vs *ex vivo* LCs (Hutter et al., 2012)	*in vitro* CD34-LCs (TGF-β1) vs *ex vivo* LCs (Hutter et al., 2012)	*ex vivo* LCs (Hutter et al., 2012) vs CD34-LCs (Lundberg et al., 2013)
Transcription Factors							
201566_x_at	ID2	1.01	-2.62	-2.60	1.07	1.08	-2.81
204198_s_at	RUNX3	-1.28	3.41	4.36	6.45	8.23	-1.89
204254_s_at	VDR	1.15	1.06	-1.08	-2.52	-2.89	2.67
1554411_at	CTNNB1	1.29	5.77	4.47	7.54	5.85	-1.31
202287_s_at	TACSTD2	-1.09	-1.66	-1.52	1.11	1.21	-1.84
201839_s_at	EPCAM	-1.34	-4.15	-3.09	1.43	1.92	-5.95
204562_at	IRF4	1.71	1.67	-1.02	-2.26	-3.85	3.77
204057_at	IRF8	1.26	-2.59	-3.27	2.95	2.34	-7.65
228837_at	TCF4	1.33	3.29	2.48	2.91	2.19	1.13
228964_at	PRDM1	1.35	-3.11	-4.20	-4.84	-6.52	1.55
212611_at	DTX4	1.07	1.21	1.13	1.45	1.36	-1.20
221841_s_at	KLF4	1.62	-15.45	-24.99	-3.56	-5.76	-4.34
232231_at	RUNX2	2.52	2.56	1.01	-9.79	-24.86	25.02
203603_s_at	ZEB2	1.66	5.41	3.26	-2.03	-3.37	10.98
232739_at	SPIB	1.19	1.08	-1.10	1.29	1.08	-1.20
209710_at	GATA2	1.50	1.73	1.16	-14.46	-21.67	25.08
Interleukins and their receptors							
202859_x_at	IL8	3.84	-23.19	-89.06	-23.17	-88.99	-1.00
215719_x_at	FAS	1.91	4.98	2.62	3.32	1.74	1.50
205067_at	IL1B	2.43	-1.14	-2.78	1.05	-2.31	-1.20
205403_at	IL1R2	2.69	-1.23	-3.31	-1.72	-4.64	1.40
209828_s_at	IL16	1.67	1.96	1.17	-1.86	-3.10	3.65
229295_at	IL17RA	2.23	8.33	3.73	-1.20	-2.69	10.04
226218_at	IL7R	2.28	34.30	15.06	2.48	1.09	13.84
204912_at	IL10RA	2.13	1.33	-1.61	-1.25	-2.67	1.66
227125_at	IFNAR2	1.47	1.35	-1.09	-4.28	-6.30	5.78
222952_s_at	TLR7	1.69	2.14	1.26	2.26	1.33	-1.05
204924_at	TLR2	2.91	6.70	2.30	-1.03	-3.00	6.90
223750_s_at	TLR10	1.41	4.48	3.17	4.02	2.84	1.12
206337_at	CCR7	1.99	1.59	-1.25	-2.35	-4.68	3.75
Signaling Molecules and Receptors							
206943_at	TGFBR1	1.20	1.65	1.98	1.85	2.22	-1.12

204832_s_at	BMPR1A	1.00	-4.09	-4.09	-1.55	-1.55	-2.64
213198_at	ACVR1B	1.111	1.94	-1.87	-1.97	-2.05	3.83
203935_at	ACVR1	1.08	-1.56	-1.69	-1.09	-1.18	-1.43
231873_at	BMPR2	-1.15	4.92	5.86	5.52	6.36	-1.12
210993_s_at	SMAD1	1.17	4.26	3.64	-1.65	-1.94	7.04
203075_at	SMAD2	-1.05	-1.72	-1.64	-1.43	-1.36	-1.20
205396_at	SMAD3	1.13	-1.02	-1.15	-1.03	-1.16	1-01
225219_at	SMAD5	-1.10	2.07	2.29	1.19	1.32	1.74
207069_s_at	SMAD6	1.89	2.42	1.28	-1.63	-3.07	3.93
1552398_a_at	CLEC12A	1.47	1.94	1.33	-7.19	-10.54	13.97
208450_at	LGALS2	2.54	1.76	-1.45	1.47	-1.73	1.19
1556209_at	CLEC2B	1.50	-2.56	-3.83	1.32	-1.14	-3.36
206682_at	CLEC10A	2.44	6.61	2.71	-2.55	-6.21	16.83
205884_at	ITGA4	4.07	14.41	3.55	2.14	-1.90	6.74
207345_at	FST	1.27	1.04	-1.22	-1.72	-2.18	1.79
204451_at	FZD1	1.68	-4.23	-7.09	1.63	-1.03	-6.91
238129_s_at	FZD2	1.32	1.72	1.30	1.16	-1.5	1.49
203705_s_at	FZD7	1.77	1.02	-1.35	1.31	-1.74	1.29
219890_at	CLEC5A	2.61	-2.44	-6.36	1.92	-1.36	-4.68
207085_x_at	CSF2RA	1.85	7.98	4.31	5.40	2.92	1.48
211286_x_at	CSF2RA	1.50	5.39	3.60	2.91	1.94	1.85
219761_at	CLEC1A	1.32	-5.55	-7.76	-5.89	-7.31	-1.06
233500_x_at	CLEC2D	1.31	1.77	1.35	2.30	1.76	-1.30
244413_at	CLECL1	1.85	-1.03	-1.89	3.54	1.92	-3.64
213475_s_at	ITGAL	2.45	3.06	1.25	-1.36	-3.36	4.20
227125_at	IFNAR2	1.47	1.35	-1.09	-4.28	-6.30	5.78
230619_at	ARNT	1.23	1.77	1.44	-1.38	-1.70	2.44
1554240_a_at	ITGAL	3.32	4.26	1.28	-1.12	-3.73	4.79
213416_at	ITGA4	3.56	7.05	1.98	1.31	-2.73	5.40
201656_at	ITGA6	-2.99	-15.62	-5.22	-3.03	-1.01	-5.16
CD antigens							
205153_s_at	CD40	1.56	2.92	-1.05	1.29	2.16	2.26
209555_s_at	CD36	1.86	28.66	15.37	-7.26	-13.53	207.93
204118_at	CD48	1.71	8.34	4.88	1.15	-1.49	7.25
201743_at	CD14	2.08	3.78	1.82	3.18	1.53	1.19
207176_s_at	CD80	1.39	4.19	3.01	1.07	-1.30	3.90
205685_at	CD86	1.17	-2.25	-2.63	3.28	2.81	-7.39
203547_at	CD4	1.26	-2.61	-3.30	1.21	-1.05	-3.15
211190_x_at	CD84	1.05	-1.14	-1.19	1.01	-1.04	-1.15
205987_at	CD1c	3.70	-2.14	-7.93	-1.71	-6.33	-1.25
210325_at	CD1a	-1.10	-1.53	1.39	-1.37	1.25	-1.12

Others							
211259_s_at	BMP7	-1.03	-1.43	-1.40	-1.56	-1.52	1.09
203084_at	TGF-β1	1.07	-1.18	-1.25	1.37	1.23	-1.54
205016_at	TGFA	2.07	1.83	-1.13	-5.22	-10.84	9.58
201130_s_at	CDH1	-1.13	1.21	1.36	1.90	2.15	-1.57
218182_s_at	CLDN1	1.29	-3.82	-4.92	-1.97	-2.53	-1.94
208712_at	CCND1	2.78	-1.12	-3.12	-2.35	-6.53	2.09
204959_at	MNDA	4.26	-7.92	-33.73	-5.75	-24.47	-1.38
1555745_a_at	LYZ	2.82	46.23	16.39	-1.51	-4.25	69.72
205569_at	LAMP3	2.22	1.31	-1.69	-1.07	-2.37	1.40
226498_at	FLT1	2.25	-3.17	-7.14	-1.19	-2.67	-2.67
206259_at	PROC	2.46	3.10	1.26	-1.74	-4.28	5.41
207808_s_at	PROS1	1.55	-6.07	-9.40	-1.85	-2.86	-3.28
205328_at	CLDN10	1.33	1.06	-1.26	-2.00	-2.66	2.11
200606_at	DSP	1.97	-7.94	-15.67	28.83	14.60	-228.80
202085_at	TJP2	1.88	-5.06	-9.53	-3.98	-7.50	-1.27
204122_at	TYROBP	1.34	1.81	1.35	2.67	1.99	-1.48
209716_at	CSF1	1.15	-1.05	-1.21	-5.69	-6.52	5.40

Up-regulated :> 1.5

Down-regulated :< 1.5

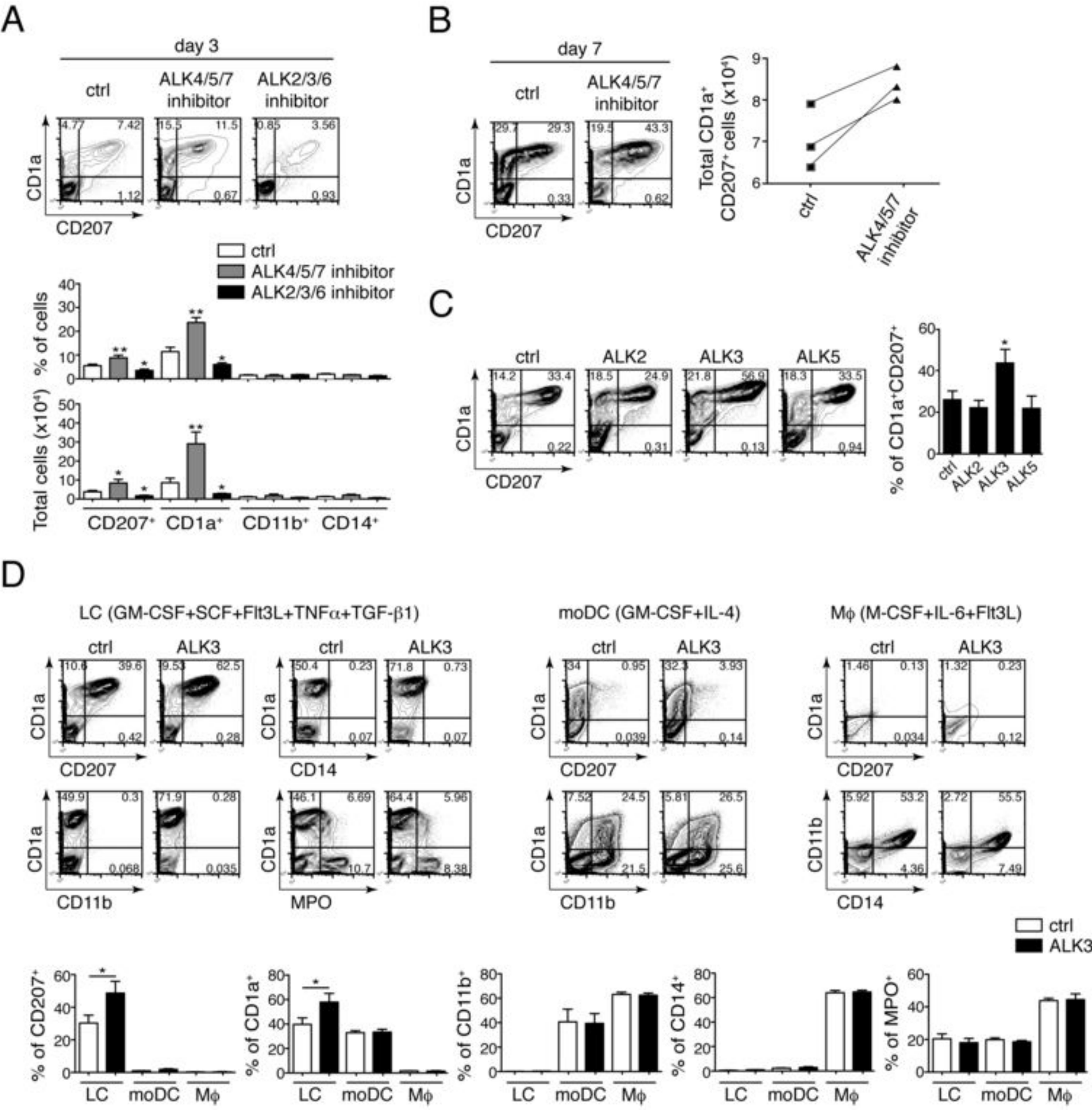
A
day 3
ctrl
ALK4/5/7 inhibitor
ALK2/3/6 inhibitor
CD1a
CD207
ctrl
ALK4/5/7 inhibitor
ALK2/3/6 inhibitor
% of cells
Total cells (x10⁴)
CD207⁺
CD1a⁺
CD11b⁺
CD14⁺
B
day 7
ctrl
ALK4/5/7 inhibitor
CD1a
CD207
Total CD1a⁺ CD207⁺ cells (x10⁴)
ctrl
ALK4/5/7 inhibitor
C
ctrl
ALK2
ALK3
ALK5
CD1a
CD207
% of CD1a⁺CD207⁺
ctrl
ALK2
ALK3
ALK5
D
LC (GM-CSF+SCF+Flt3L+TNFα+TGF-β1)
moDC (GM-CSF+IL-4)
Mϕ (M-CSF+IL-6+Flt3L)
ctrl
ALK3
CD1a
CD207
CD14
CD11b
MPO
ctrl
ALK3
% of CD207⁺
% of CD1a⁺
% of CD11b⁺
% of CD14⁺
% of MPO⁺
LC
moDC
Mϕ

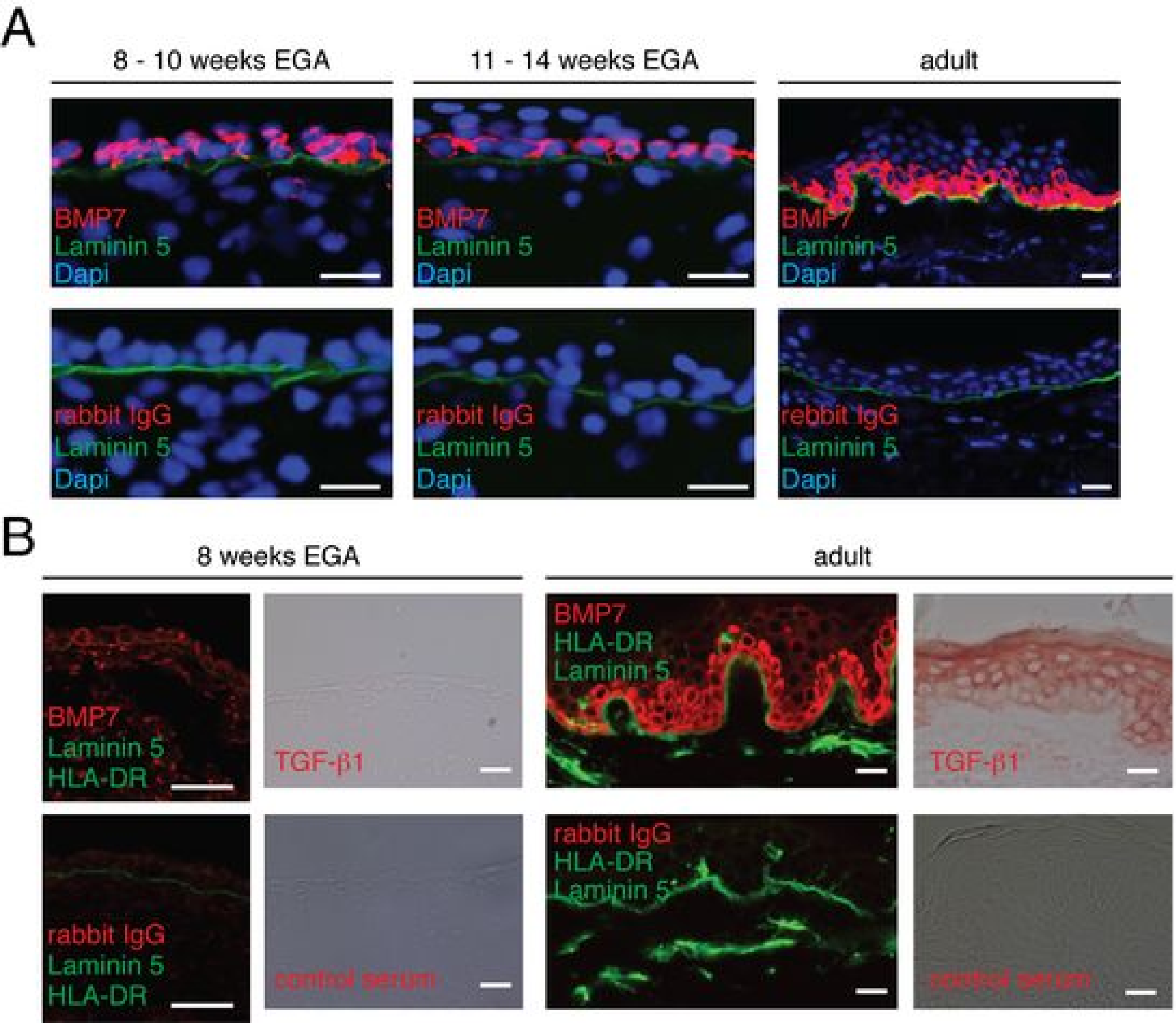
A
8 - 10 weeks EGA
11 - 14 weeks EGA
adult
BMP7
Laminin 5
Dapi
BMP7
Laminin 5
Dapi
BMP7
Laminin 5
Dapi
rabbit IgG
Laminin 5
Dapi
rabbit IgG
Laminin 5
Dapi
rebbit IgG
Laminin 5
Dapi
B
8 weeks EGA
adult
BMP7
Laminin 5
HLA-DR
TGF-β1
BMP7
HLA-DR
Laminin 5
TGF-β1
rabbit IgG
Laminin 5
HLA-DR
control serum
rabbit IgG
HLA-DR
Laminin 5
control serum

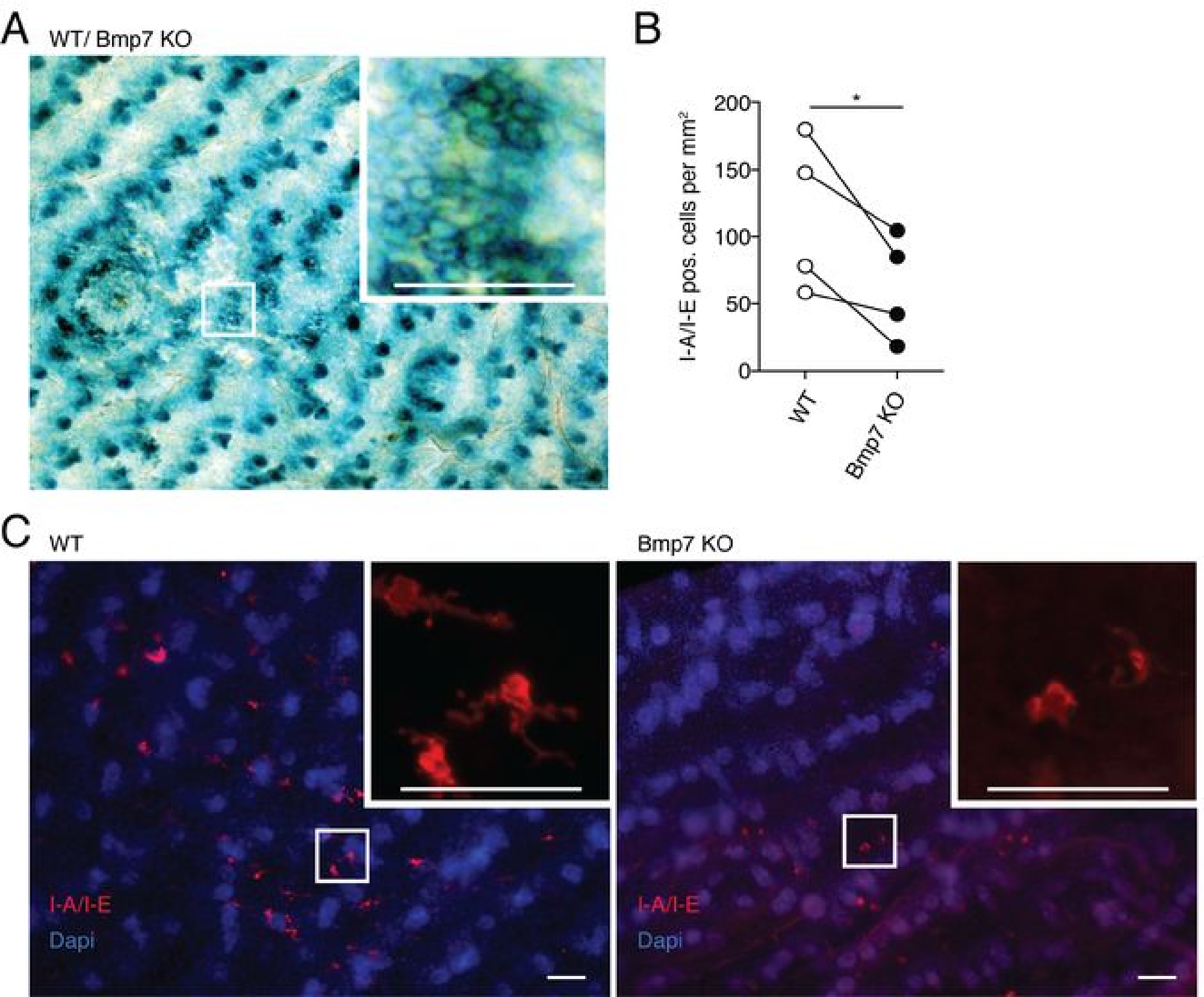
A
WT/ Bmp7 KO
B
I-A/I-E pos. cells per mm²
200
150
100
50
0
*
WT
Bmp7 KO
C
WT
Bmp7 KO
I-A/I-E
Dapi
I-A/I-E
Dapi

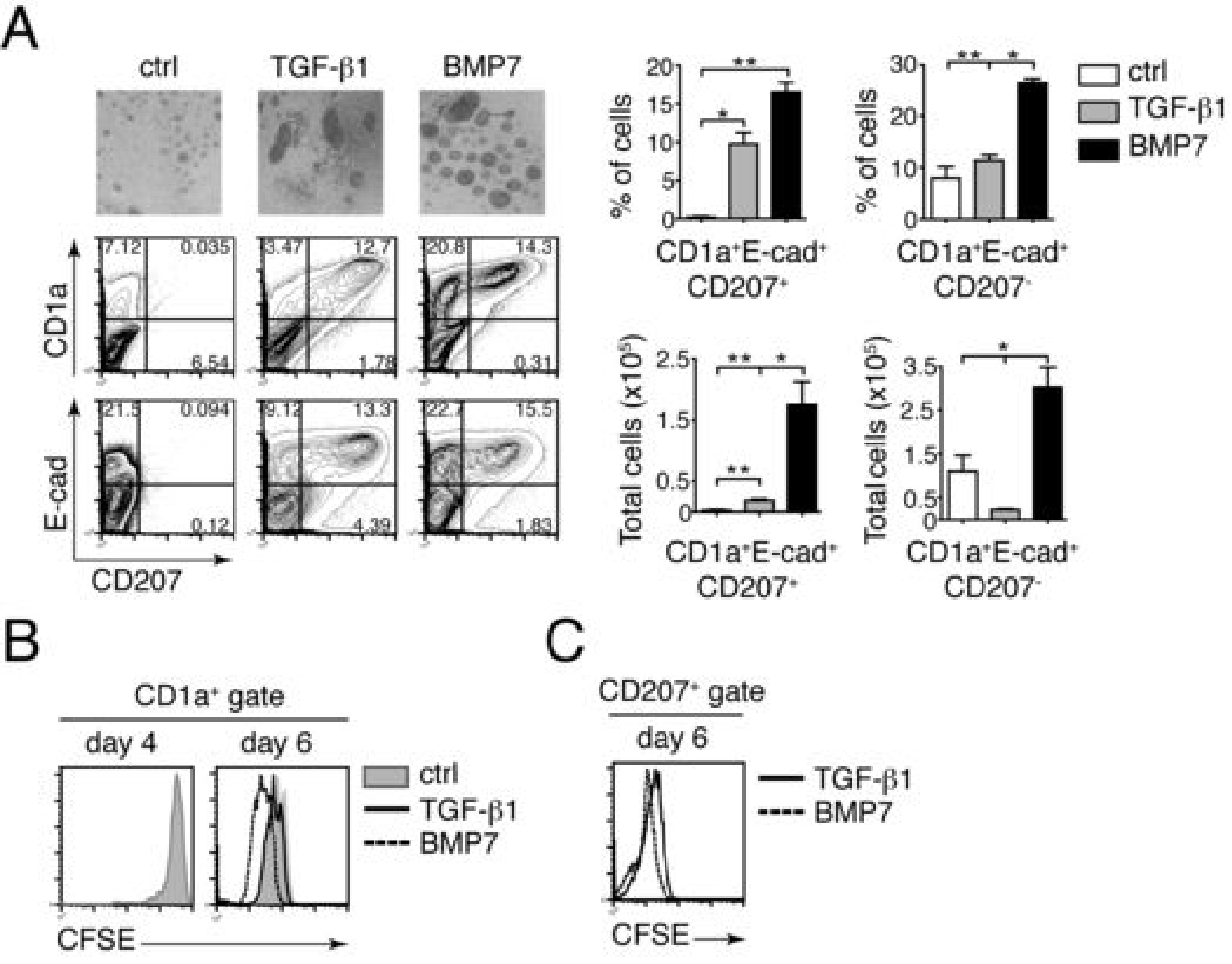
A
ctrl
TGF-β1
BMP7
CD1a
E-cad
CD207
7.12
0.035
6.54
3.47
12.7
1.78
20.8
14.3
0.31
21.5
0.094
0.12
9.12
13.3
4.39
22.7
15.5
1.83
% of cells
CD1a+E-cad+ CD207+
CD1a+E-cad+ CD207-
ctrl
TGF-β1
BMP7
Total cells (x10^5)
B
CD1a+ gate
day 4
day 6
CFSE
C
CD207+ gate
day 6
CFSE

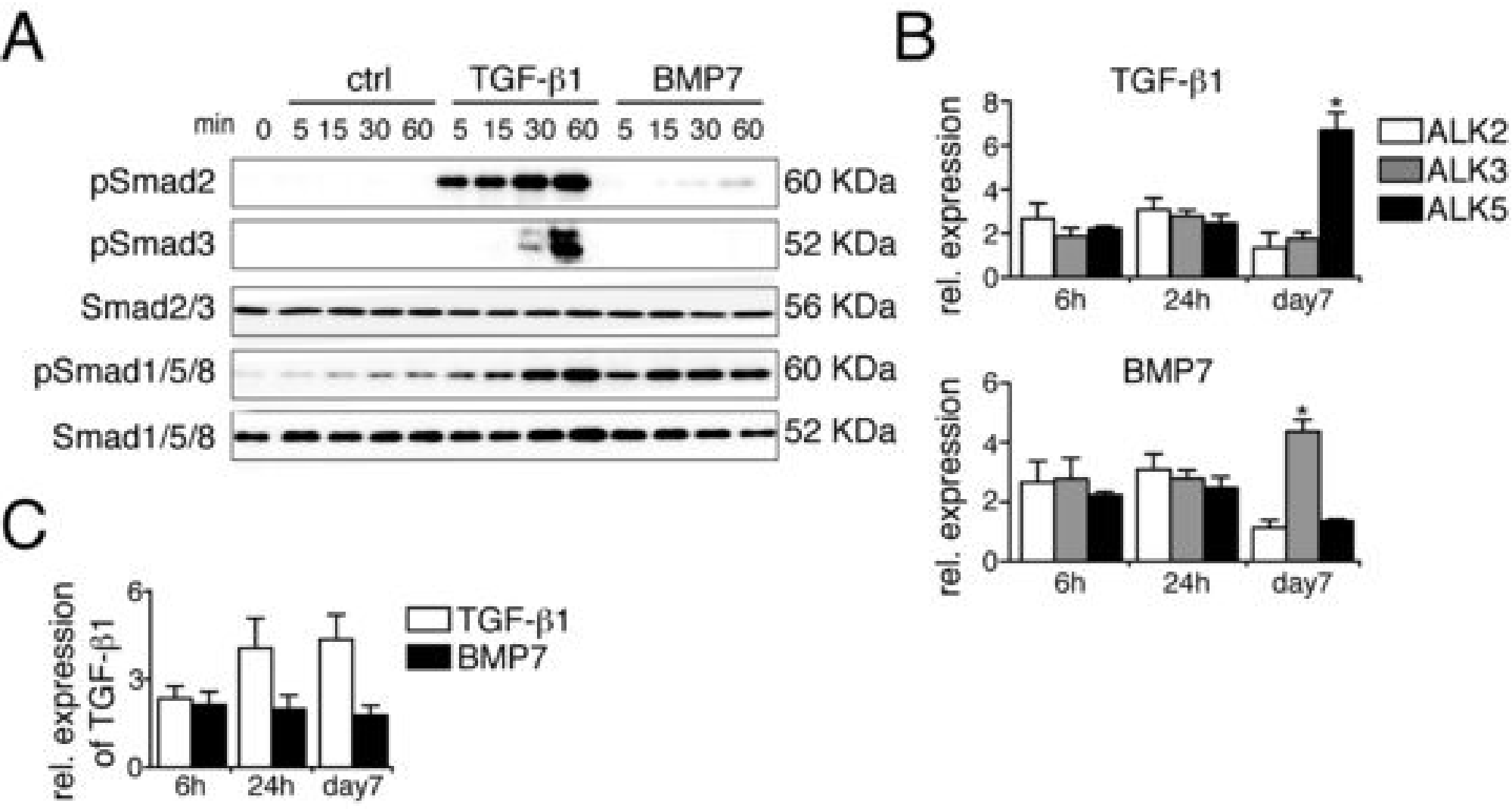
A
ctrl
TGF-β1
BMP7
min 0 5 15 30 60 5 15 30 60 5 15 30 60
pSmad2
60 KDa
pSmad3
52 KDa
Smad2/3
56 KDa
pSmad1/5/8
60 KDa
Smad1/5/8
52 KDa
B
TGF-β1
rel. expression
ALK2
ALK3
ALK5
6h
24h
day7
BMP7
rel. expression
6h
24h
day7
C
rel. expression of TGF-β1
TGF-β1
BMP7
6h
24h
day7

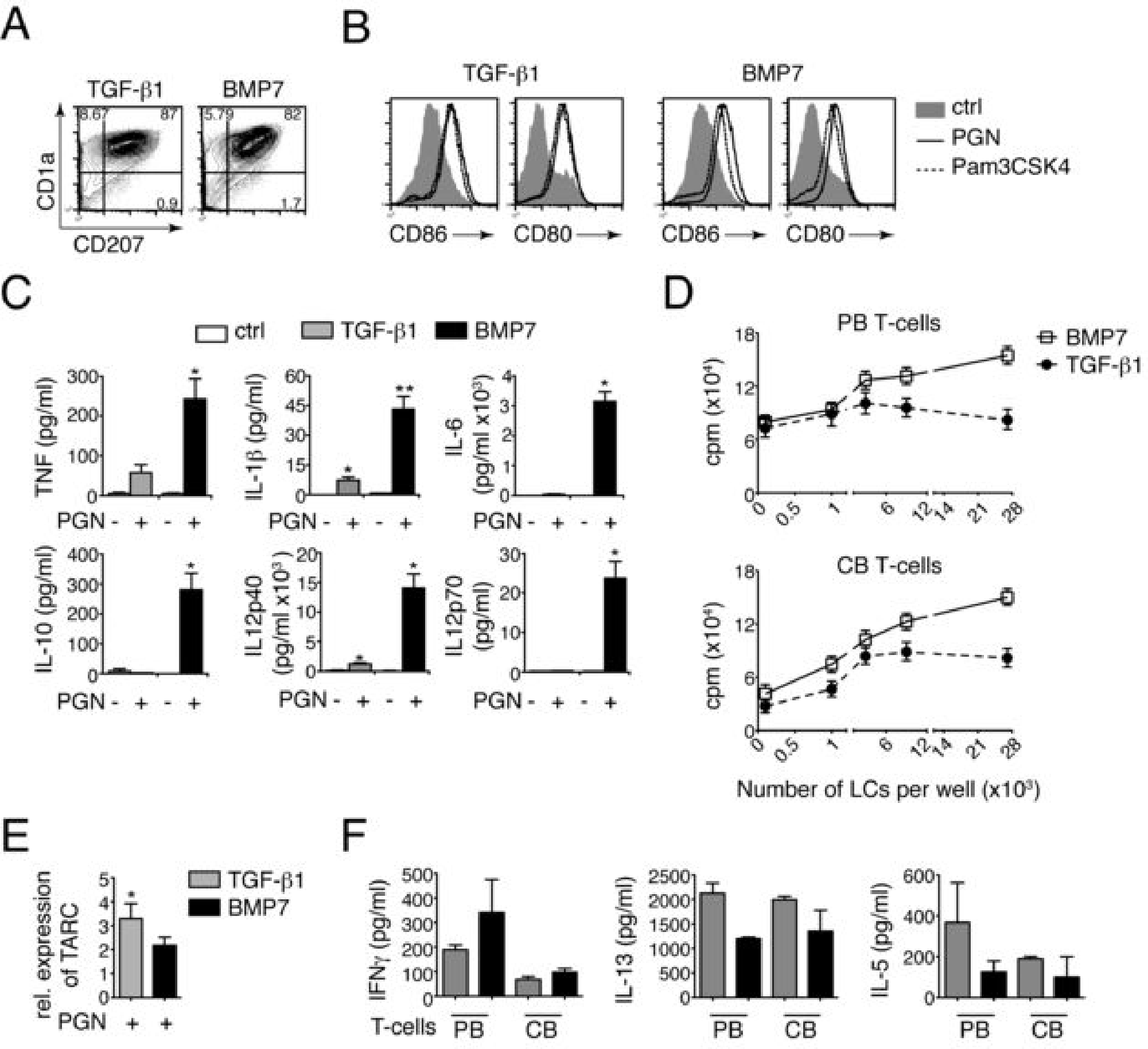
A
TGF-β1
BMP7
8.67
87
0.9
5.79
82
1.7
CD1a
CD207
B
TGF-β1
BMP7
ctrl
PGN
Pam3CSK4
CD86
CD80
CD86
CD80
C
ctrl
TGF-β1
BMP7
TNF (pg/ml)
IL-1β (pg/ml)
IL-6 (pg/ml x10³)
IL-10 (pg/ml)
IL12p40 (pg/ml x10³)
IL12p70 (pg/ml)
PGN - + - +
D
PB T-cells
CB T-cells
BMP7
TGF-β1
cpm (x10⁴)
Number of LCs per well (x10³)
E
TGF-β1
BMP7
rel. expression of TARC
PGN + +
F
IFNγ (pg/ml)
IL-13 (pg/ml)
IL-5 (pg/ml)
T-cells
PB
CB

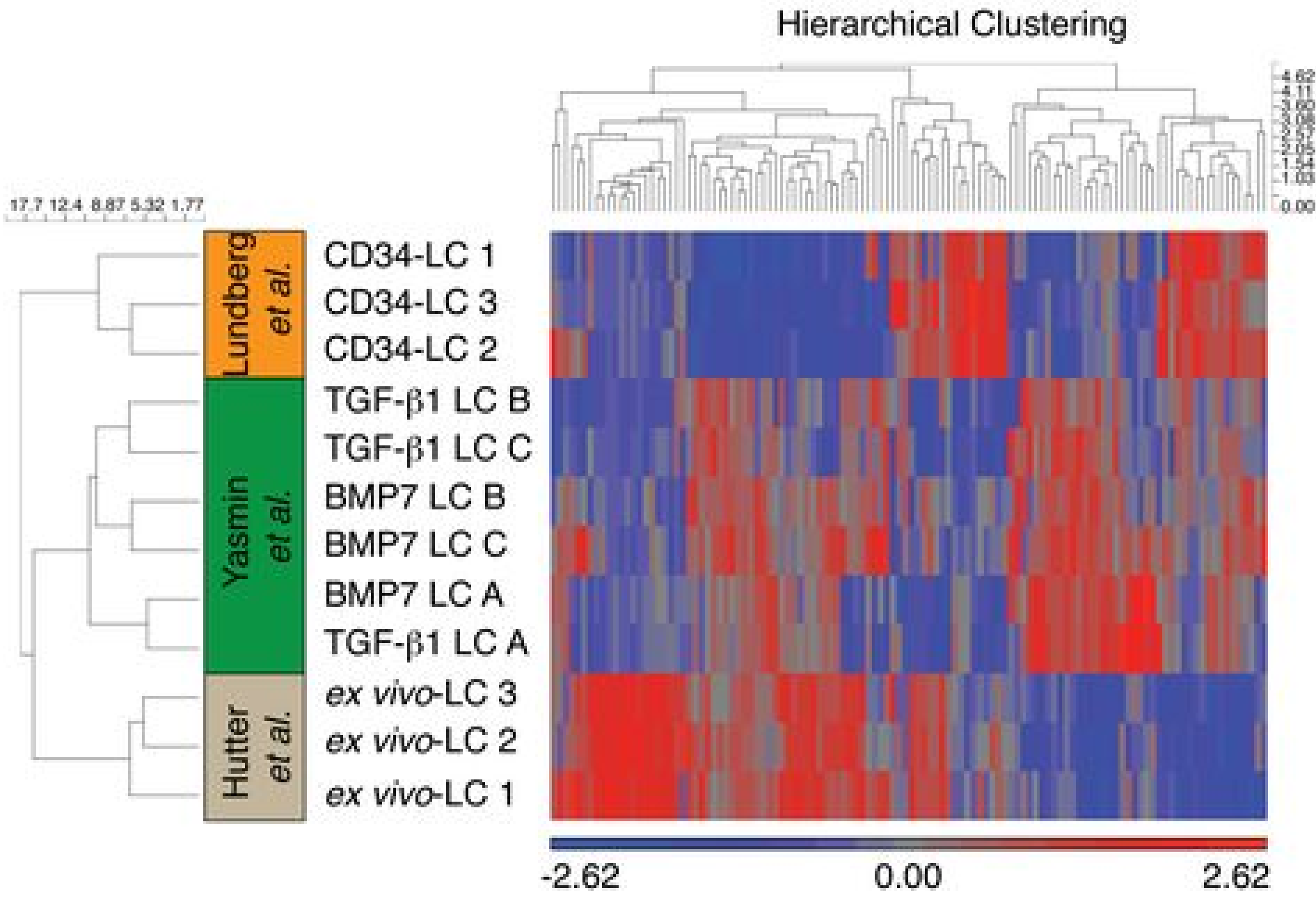
Hierarchical Clustering
17.7 12.4 8.87 5.32 1.77
Lundberg et al.
Yasmin et al.
Hutter et al.
CD34-LC 1
CD34-LC 3
CD34-LC 2
TGF-β1 LC B
TGF-β1 LC C
BMP7 LC B
BMP7 LC C
BMP7 LC A
TGF-β1 LC A
ex vivo-LC 3
ex vivo-LC 2
ex vivo-LC 1
-2.62
0.00
2.62

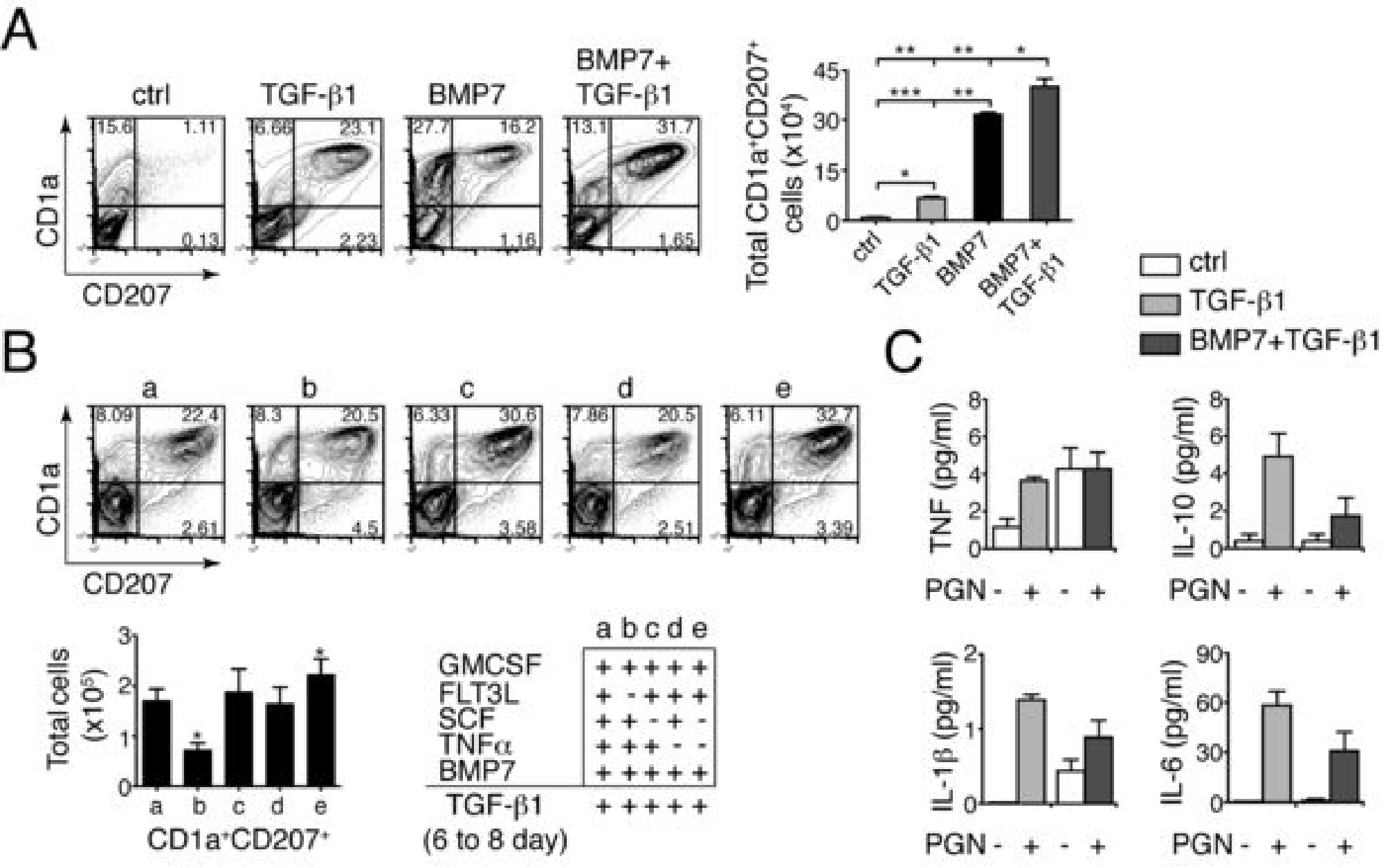
A
ctrl
TGF-β1
BMP7
BMP7+ TGF-β1
CD1a
CD207
15.6
1.11
0.13
6.66
23.1
2.23
27.7
16.2
1.16
13.1
31.7
1.65
Total CD1a+CD207+ cells (x10⁴)
45
30
15
0
ctrl
TGF-β1
BMP7
BMP7+ TGF-β1
B
a
b
c
d
e
8.09
22.4
2.61
8.3
20.5
4.5
6.33
30.6
3.58
7.86
20.5
2.51
8.11
32.7
3.39
Total cells (x10⁵)
CD1a+CD207+
GMCSF
FLT3L
SCF
TNFα
BMP7
TGF-β1
(6 to 8 day)
C
ctrl
TGF-β1
BMP7+TGF-β1
TNF (pg/ml)
IL-10 (pg/ml)
IL-1β (pg/ml)
IL-6 (pg/ml)
PGN - + - +